Imperial College London

Modelling density-dependent *Anopheles* population dynamics and its implications for gene-drive programmes

Oliver Simmons

Primary Supervisor – Dr Penny Hancock

Co-supervisor – Dr Ace North

MRes in Biomedical Research at Imperial College London

Date of Submission: 04/03/2024

Table of Contents

Statements of Originality 3
Acknowledgements 3
Abbreviations 3
Abstract 4
Introduction 5
Gene Drives 6
Modelling *Anopheles* 7
The Density-Dependence Assumption 9
Aims and Objectives 14
Methods 15
The Nisbet and Gurney Model 15
Modifications to Nisbet and Gurney's model 20
Incorporating a Pupal Class 20
Incorporating Density-Dependent Fecundity 21
Parameterizing the model to represent *Anopheles gambiae* populations 23
Coding 25
Sensitivity Analysis 26
Predicting the Impacts of Gene-drive Interventions 27
Comparison with other Models of Larval Density-dependence 28
Uncertainty Analysis 29
Results 30
A Modified Model representing Multiple Density-dependent Demographic Traits 30
Predicting the Population Dynamics of *Anopheles gambiae* 32
Sensitivity to Female Fecundity and Larval Mortality Parameters 33
Effects of Density-independent Larval Mortality on Density-dependent Demographic Traits 36
Predicting the Impacts of a Suppression Gene Drive 37
Discussion 42
Future Work 46
Conclusion 47
References 48
Supplementary Materials 51
Algorithm used to classify the equilibrium solution of the Modified Nisbet and Gurney model used in the project and to calculate the long-term value of its states 56
Parameter values used in the model comparison 57
Supplementary Figures 58

Statements of Originality

I certify that this thesis, and the research to which it refers, are the product of my own work, conducted during the year of the MRes in Biomedical Research at Imperial College London. Any ideas or quotations from the work of other people, published or otherwise, or from my own previous work are fully acknowledged in accordance with the standard referencing practices of the discipline.

The model used in this project was based on a model developed by Nisbet and Gurney in their 1983 paper "The Systematic Formulation of Population Models for Insects with Dynamically Varying Instar Duration"[(1)]. This project contains a description of a specific case of their model (Methods) and a derivation of an equilibrium solution for a modified version of their model (Supplementary Materials), both of which draw heavily from this paper. Two other models of *Anopheles* population dynamics were used for a model comparison. These were White et al.'s model from their 2011 paper "Modelling the impact of Vector Control Interventions on *Anopheles gambiae* population dynamics"[(2)] and Hancock and Godrfay's model from their 2007 paper "Application of the lumped age-class technique to studying the dynamics of malaria-mosquito-human interactions"[(3)].

I hereby confirm that the submitted work is entirely my own and I have not used the service of any generative Artificial Intelligence (AI) to generate any content. I acknowledge that doing so will constitute an examination offence and will be formally investigated as such.

Acknowledgements

Thanks to Dr Penny Hancock for all her help during the past 5 months, and for replying to all my emails. Her wisdom and advice have been invaluable, and without which the quality of this project would have been much diminished. Thanks also to Dr Ace North for his advice and help during the project.

Abbreviations

DDE - Delay Differential Equation, EIR - entomological inoculation rate, IRS – Indoor Residual Spraying (of insecticides), ITN – Insecticide Treated Bed-Net, LHS = Latin Hypercube Sample, LLIN – Long Lasting Insecticide-treated bed-Net, ODE – Ordinary Differential Equation, SP - Sulphadoxine-Pyrimethamine, WHO – World Health Organization

Abstract

Suppression gene drives, where a modified gene is spread through a mosquito population, reducing the number of mosquitoes, have been proposed as a method of malaria control. It is not known how gene drives will behave in wild populations, and the extent of suppression may depend on density-dependent changes in population growth rates. Different models of mosquito population dynamics make different assumptions about density-dependence, but both semi-field and laboratory-based studies suggest additional density-dependent processes that are not captured in current models.

I developed a delay-differential equation model of *Anopheles* mosquito population dynamics that included density-dependence in larval-to-pupal development time and female fecundity. For parameter values representative of *Anopheles gambiae*, the model produced equilibrium values of density-dependent traits within experimentally observed ranges. A sensitivity analysis of the model identified that, in different areas of the parameter space, the model exhibits stable equilibria, extinction, and oscillations. The impact of a suppression gene drive on the *Anopheles* population was simulated by assuming females homozygous for a suppression gene drive are sterile and unable to bite. The model predicted that as the number of mosquitoes homozygous for a suppression gene drive increased, the abundance of the adult mosquito population increased, but the number of adult females able to spread malaria decreased.

The model's predictions were compared to those of two other mosquito population dynamics models that assume density dependence acts only on larval mortality. The three models gave contrasting results on the impact of suppression gene drives, with the greatest difference between the models occurring when the gene drive was homozygous in 74% of the population. At this point, the predicted decrease in the number of adult females able to spread malaria ranged from 35.3% to 76.4%. I discuss how structural differences between the three models leads to this discrepancy. Assumptions about density-dependence can have a large impact on the suppression effects of gene drives. This uncertainty needs to be considered and communicated to policy makers if gene drives are to be implemented in the field.

Introduction

Malaria remains a significant problem worldwide. Considerable advancements over the last 20 years, including vastly increased coverage of insecticide treated bed-nets (ITNs), long-lasting insecticide treated bed-nets (LLINs) and indoor residual spraying of insecticides (IRS), and better access to chemoprevention, led to a 40% reduction in clinical malaria incidence in Sub-Saharan Africa (where 95% of malaria cases occur[4]) between 2000 and 2015[5]. Despite these advancements, progress towards elimination has stalled in recent years, with malaria case incidence increasing marginally from 57 per 1000 people at risk in 2019 to 58.4 per 1000 people at risk in 2022, and deaths due to malaria rising from 568,000 in 2019 to 608,000 in 2022[6]. This means that, as per the World Malaria Report 2023[6], current incidence levels are 123% higher and current mortality levels 117% higher than needed to reach the 2025 targets of the World Health Organization (WHO) Global Technical Strategy for malaria 2016-2030[7].

The efficacy of the current suite of interventions used to fight malaria is threatened by growing insecticide resistance, growing drug resistance and new developments in the distribution of malaria vectors. ITNs and LLINs were estimated to be responsible for 68% of the clinical case incidence reduction seen in Africa between 2000 and 2015[5], and the increasing resistance of *Anopheles* mosquitoes (malaria's vectors[4]) to the insecticides used in ITNs and LLINs is a considerable problem[6, 8, 9]. *Plasmodium falciparum*, the parasite that causes the majority of malaria cases in Africa[10, 11], has, in some countries, been found to be increasingly resistant to antimalarial drugs such as sulphadoxine-pyrimethamine (SP) and artemisinin[12, 13]. Both SP and artemisinin are important drugs in malaria chemoprevention programmes across the world[14], so any decline in their efficacy could have significant negative consequences. Any intervention efficacy issues could also exacerbate the problems caused by the invasion of the malaria vector *Anopheles stephensi* into East Africa. *Anopheles funestus* and species of the *Anopheles gambiae s.l.* complex, which are responsible for the majority of malaria transmission in Africa[15], live mostly in rural areas, so the introduction of *An. stephensi*, an urban vector[6], into Africa could lead to millions more at risk. It is crucial that other interventions are developed that can not only fill these gaps, but also reverse the trend in cases and mortality seen in recent years.

Gene Drives

One such intervention that has been proposed is the introduction of gene drives into Africa's *Anopheles* populations. A "gene drive" is the name given to a process where a specific gene is introduced to, and then spreads through, a population via super-Mendelian inheritance dynamics (which is where a gene spreads to more than 50% of offspring)[16, 17]. CRISPR-Cas9 gene editing technology is used to modify a gene to make it selfish, causing homologous chromosomes not containing the modified gene to be cleaved at the target locus and then repaired by copying the modified gene into the cleavage site, using the undamaged (modified-gene-containing) chromosome as a template. This converts individuals that are heterozygous with respect to the modified gene into homozygotes, biasing inheritance towards progeny that carry the modification[16, 18]. This process can be leveraged to spread a specific genetic modification through an entire population, rendering members either infertile or unable to spread certain diseases[16]. The process does have drawbacks, as individuals heterozygous for an edited gene often experience a fitness cost when compared with the wild-type population, meaning the gene's spread slows, and resistance to edited genes can develop within a population, stopping their spread entirely[16]. Nevertheless, it is possible to overcome these issues[16, 19, 20].

The gene drives currently being studied that have been proposed to combat malaria fall into one of two categories: suppression gene drives or replacement gene drives. The aim of a suppression gene drives is to either eliminate the mosquito population, thereby stopping the transmission of malaria, or drive the mosquito population to such a low level that malaria transmission cannot be sustained. This is done by inducing a recessive homozygous fitness cost, decreasing the number of mosquitoes born each generation[18], which leads to a reduction in malaria transmission. Additionally, some suppression gene drives have been developed that render female mosquitoes both sterile and unable to bite (meaning they are unable to spread *P. falciparum*, reducing malaria transmission further)[19]. On the other hand, the idea behind a replacement gene drive is to replace the wild-type *An. gambiae* population with one that carries a gene that renders mosquitoes unable to spread the *P. falciparum* parasite[21], reducing malaria transmission without wiping out the entire population.

Due to the concerns around gene drives identified by various risk assessments, such as the possibility of an edited gene being transmitted to other species and the potential negative impacts of eliminating an entire vector species on human health, animal health and biodiversity[22-24], multiple phases of testing, risk assessments, community engagement and regulatory decisions are needed before field testing can be undertaken[23]. In the meantime, being able to mathematically model the spread of a gene drive is vital, as it can help us to understand the potential impacts of the gene drive on the *An. gambiae* population, the effectiveness of the gene drive at reducing malaria incidence in the chosen region, and the most effective way to implement the gene drive, in terms of release population, location and timing[22, 23]. Such models need to incorporate both a model for *Anopheles* ecology and population dynamics, and a mathematical model for malaria transmission between humans and mosquitoes. The assumptions underpinning these models can have significant consequences on their results, so understanding these assumptions and the motivations behind them is crucial.

Modelling *Anopheles*

Modelling the population dynamics of *Anopheles* mosquitoes, and mosquitoes in general, is often done using a system of differential equations, where the different states of the model represent the different stages in the mosquito's life cycle. Beyond this, model design varies depending on the author's assumptions and needs, and can be as simple or as complex as desired (however models as intricate as that of Depinay et al.[25], which incorporates both the biological processes inside the mosquito and the water dynamics in the larval habitat, are rarely used). For example, after hatching, *Anopheles* goes through four larval instar stages before pupating, after which they emerge as an adult[26], and the choice of which of these life-stages to explicitly model varies. Hancock and Godfray[3] model mosquitoes as either eggs, larvae, pupae or adults, whereas White et al.[2] model mosquitoes as either Early Larval (a state which encompasses the first two larval instar stages), Late Larval (encompassing the latter two larval instar stages), pupal or adult, and North and Godfray[27, 28] use only two classes; mosquitoes are classified as either juvenile (which encompasses all larval stages and the pupal stage) or adults.

One method to model Anopheles population dynamics is delay-differential equations (DDEs). This method is used by Hancock and Godfray[3], who used a deterministic "lump-aged class" model, where the time taken to move through the egg, larval and pupal stages is fixed. Only the larval and adult states are explicitly modelled, and delay-differential equations are used to capture the developmental period required for larvae to become adults[3]. A discrete time version of this model structure was also used by Deredec et al.[29] in 2011 to study the requirements for various theoretical gene drives to be successful. Deredec et al.'s model formulation was also used by Sanchéz et al. in their first version of "MGDrivE"[30], a model used to simulate the dynamics of gene drives in mosquito populations, and by Marshall et al.[31]. The delay-differential approach differs from that of White et al.[2], who use a deterministic ordinary differential equation (ODE) structure with fixed development rates between stages (meaning, for example, that larval development time is gamma-distributed[2]). The White et al.[2] model is used to represent mosquito dynamics in the "malariasimulation" model[2, 32-37], a widely used open-source model of malaria transmission dynamics (although in "malariasimulation", the model becomes stochastic and is written in terms of a system of Kolmogorov forward differential equations[36]). Wu et al.[38] use a similar approach to White et al.[2] in the second version of "MGDrivE 2" to incorporate time-varying larval development rates and mortality (where both are affected by seasonality)[38], and "MGDrivE 2" has subsequently been used by Carballar-Lejarazú et al.[20] to model the effectiveness of two candidate parasite-suppression gene drives on *An. gambiae* and *An. coluzzii* on Grande Comore.

More recent papers aiming to model the spatial spread of gene drives through a large country or region during a field trial have tended to use stochastic individual-based models, where the probability of individual mosquitoes surviving and moving between states is modelled. This was the approach taken by North and Godfray[27] in 2018 and by North et al.[28] in 2020, who studied the spatial spread of *An. gambiae* in Burkina Faso, and the effects of a gene drive affecting female *An. gambiae* fertility in Burkina Faso, respectively. Eckhoff et al.[39] also used this approach (in an adaptation of an earlier model developed by Eckhoff[40]) to study the spread of a driving-Y gene drive in Tanzania and Nigeria. Additionally, Metchanun et al. [41] used a malaria transmission dynamic model known as "EMOD", which incorporates Eckhoff's original model[40], to estimate the effectiveness of a driving-Y gene-drive in reducing malaria in provinces in the

Democratic Republic of the Congo[42]. Other approaches to modelling the population dynamics of *Anopheles* mosquitoes in gene drive models include using reaction-diffusion equations to model the spread of the gene drive through the population[43], only modelling adult male and female mosquitoes [44], or forgoing mosquito population dynamics entirely and instead using population genetic approaches to model the spread of the new, modified allele through a population containing only wild-type alleles[45, 46].

The Density-Dependence Assumption

An assumption made in the papers discussed above, which all in some way incorporate the larval stage of *Anopheles*' life cycle, is that larval populations are regulated by density dependence, and, more specifically, regulated by the density dependent mortality of larvae. This is modelled by splitting larval mortality into non-density-dependent mortality, which occurs at a constant per capita rate, and density dependent mortality, which occurs at a per capita rate proportional to the larval density[2, 3, 20, 29, 30, 38]. Within this structure, the assumption can take different forms; Hancock and Godfray[3] use a simple linear term to incorporate this density dependence, whereas White et al.[2] incorporate density dependent larval mortality through a time-varying carrying-capacity which changes according to recent rainfall. A small number of studies have considered models in which density dependence acts on other demographic and ecological processes, such as Depinay et al.[25], who also modelled adult weight (and subsequently fecundity) as density dependent, and Eckhoff et al.[39], who chose to model density-dependent habitat selection for oviposition, which has been seen experimentally[47].

Any assumption of density dependence is particularly important when studying the effects of gene-drives, especially gene-drives for population suppression, as density dependent characteristics can significantly affect the extent to which populations can be suppressed. For example, a gene-drive affecting female fertility could cause the population to rebound in size due to density-dependent increases in the population growth rate. If the population then increases to a larger size than before, the population would be said to be demonstrating overcompensatory behaviour, and similarly, if it increased to a smaller size then before, undercompensatory behaviour. Additionally, if density dependence acts on demographic processes other than larval mortality, then reducing the *An. gambiae* population could have unforeseen consequences. It is

therefore crucial to both understand the nature of *Anopheles*' density dependence further, and to critically assess the assumptions made about its density dependence in previous papers[21].

I have reviewed the literature on experimental studies looking at the effects of larval density dependence on the life-history characteristics of *Anopheles* mosquitoes. Their results, which are summarised in Table 1, are discussed below. The two main types of study carried out were laboratory-based studies[48-55], where larvae are reared in a container of water in a laboratory and are provided with food (often the fish food *Tetramin*), and semi-field studies[56-59], where either a container containing the larvae is placed in a larval habitat, for example a lagoon[59] or swamp[60], or a container is placed in the ground and filled with mud and water from a nearby source, to simulate a puddle-like larval habitat[56-58]. Of these two study types, semi-field studies test larvae at much lower densities, but are an improvement over laboratory-based studies, as they provide growing conditions more similar to those found in real-life habitats. The majority of studies, both field and laboratory based, investigated the effects of density-dependence on larval development time to the pupal stage, on larval survivorship to the pupal stage, and on some measure of size, be it adult mass, adult wing length or larval or pupal size. It should however be noted that studies have tended to look at the effects of density dependence over a single generation of larvae, not consecutive generations, which means that we are unable to assess longer term density-dependent impacts when generations of mosquitoes overlap.

Among the laboratory-based studies, the majority found that larval development time is density dependent, and that increasing larval density in turn increases larval development time (Table 1). However, Timmermann and Briegel[55] did not observe this at every density treatment for *An. albimanus*, Tsila et al.[52] found conflicting results and Lyimo et al.[48] found that development time decreased with increased density. The majority of laboratory studies also found that survival from the first instar larval stage to either the pupal or adult stage was density dependent, and that survival decreased (i.e., mortality increased) as larval density increased (Table 1). Exceptions to this include studies by Lyimo et al.[48] and Gilles et al.[51], whose results seemed to impacted by, respectively, temperature and food levels, and studies by Schneider et al.[49] and Timmermann and Briegel[55], which both observed the phenomenon in some species of *Anopheles* but

not others. Finally, with respect to either larval, pupal or adult body size, there was broad consensus among the laboratory studies that increased density causes a decrease in body size (Table 1), with all studies finding this apart from Lyimo et al.[48].

In general, differing study methodologies make comparing the results of the laboratory-based studies difficult. For example, the highest density used by Tsila et al.[52] is significantly higher than the highest density in any other study (Table 1), and the authors note that high mortality at the start of the experiment at this density could have caused the larvae who survived this period to actually experience low density growth[52]. Lyimo et al.'s[48] choice to vary temperature as well as density also poses issues in light of temperature's impact on *An. gambiae s.s.* larvae survival[61, 62], and this may be the reason for that study's often conflicting results. Another major difference between the studies was their decision to either hold food constant per larva (meaning higher density treatments received more food) or to keep the amount of food the same regardless of the number of larvae (see Table 1). It is assumed that density-dependent food competition plays a major role in the density dependence of mosquito larvae, and subsequently this could only have been observed in the laboratory studies who made the second study design choice (Gilles et al.[51], Tchuinkam et al.[50] and Yadav et al.[53]). This means that the density dependence observed in the food-constant-per-larva studies may be due to other factors (Ng'habi et al.[54] theorised that *Anopheles* larvae, like *Aedes* mosquito larvae, may secrete a chemical at high densities that affects larval growth).

Of the semi-field studies, all five studies agree that increasing larval density increases larval development time[56-60] (Table 1). Of the four semi-field studies that looked at the impact of larval density on mosquito size (Njunwa[56] did not study this), Gimnig et al.[57], Munga et al.[60] and Muriu et al.[58] found that adult wing length decreased as density increased, and Russell et al.[59] noticed visually that larval and pupal size decreased. As with the laboratory studies, the results were more mixed when looking at the effects of density on larval survivorship. Of the semi-field studies, two found that survivorship decreased with density, whereas Gimnig et al.[57] and Munga et al.[60] both found no effect of larval density on survivorship, and Njunwa[56] found that survival only decreased with increasing density when all larvae were inputted into the cage at the same time, and not if their imputation was staggered. Compared to the laboratory studies, the

interpretation of the semi-field studies is more straightforward; they do not add mosquito feed to the habitat, so there is no discrepancy about whether to add constant mosquito feed per larva or per habitat.

Study	Lyimo et al. 1992	Timmermann and Briegel 1993	Njunwa 1993	Schneider et al. 2000	Gimnig et al. 2002	Ng'habi et al. 2005	Munga et al. 2006	Tchuinkam et al. 2011	Gilles et al. 2011	Tsila et al. 2011	Muriu et al. 2012	Russell et al. 2016	Yadav et al. 2017
Type	Lab	Lab	Semi-field	Lab	Semi-field	Lab	Semi-field	Lab	Lab	Lab	Semi-field	Semi-field	Lab
Species/subspecies	An. gambiae s.s.	An. gambiae s.s, An. stephensi & An. albimanus	An. gambiae s.l.	An. gambiae s.s. & An. arabiensis	An. gambiae s.s.	An. gambiae s.s.	An. gambiae s.l.	An. gambiae s.s.	An. arabiensis	An. gambiae, unclear if s.l. or s.s.	An. gambiae s.s.	An. farauti	An. stephensi
Food constant per larva or per ml?	Per larva	Per container	-	Per larva	-	Per larva	-	Per container	Per container	Per larva	-	-	Per container
Density range	0.1-0.4 larva/ml or 0.5-2 larva/cm^2	0.208- >2.5 larva/cm^3 (An. albimanus), 0.208-3.125 larva/cm^3 (An. gambiae s.s, 0.104- >1.25 larva/cm^3 (An. stephensi)	0.016-0.024 larva/cm^3(however partially submerged so unsure of true volume)	0.1-0.4 larva/ml or 0.5-2 larva/cm^2	0.02-0.2 larva/ml or 0.033-0.33 larva/cm^2	0.1-0.3 larva/ml	0.021-0.10 larva/cm^2, volume unclear (between max 0.008-0.02 larva/ml and min 0.0014-0.0069 larva/ml)	0.3-2.4 larva/cm^2 or 0.3-1.6 larva/ml	0.25-4 larva/ml	0.5-15 larva/ml	0.033-0.53 larva/cm^2 or 0.0033-0.053 larva/cm^3	0.026-0.26 larva/cm^2	0.1-1 larva/ml
Effect of increasing larval density on:													
Larval Development Time	Decreased	Increased for An. gambiae s.s and An. stephensi, decreased then increased for An. albimanus	Increased for instar stages ii, iii and pupae, no effect for stages i and iv	-	Increased	-	Increased	Increased	Increased	Increased then decreased	Increased	Increased	Increased
Larval Survival	Temperature dependent	Decreased for An. stephensi, increased then decreased for An. gambiae s.s. and An. albimanus	Decreased for single input, no effect for multiple inputs	Decreased for An. gambiae, no effect for An. Arabiensis	No effect	Decreased	No effect	Decreased	Decreased except at high food levels	Decreased	Decreased	Decreased	Decreased
Adult Mass	Temperature dependent	-	-	-	Decreased	-	-	-	Decreased	-	-	-	Decreased
Adult Wing Length	Temperature dependent	Decreased for all 3 species	-	-	-	-	Decreased	-	-	Decreased then increased	Decreased	-	-
Pupal Mass	-	-	-	-	-	-	-	-	-	Decreased then increased	-	-	-
Larval and Pupal Size	-	-	-	-	-	-	-	-	-	-	-	Decreased (visually)	-
Larval Length	-	-	-	-	-	-	-	Decreased	-	-	-	-	-
Adult Male Mating Competitiven-ess	-	-	-	-	-	Decreased	-	-	-	-	-	-	-

Table 1: Results of the experimental studies on the density dependence of Anopheles larvae.

Further evidence in support of density-dependent life-history characteristics is the fact that Takken et al.[63] used density dependence to vary the body size of their adult females when looking at the effects of body size on adult females' host-seeking. Additionally, modelling work done by Russell et al.[64] on *An. gambiae s.l.* and by Ngowo et al.[65] on *An. funestus* found that model performance improved when density-dependent mosquito growth, in the case of Russell et al.[59], and mortality, in the case of Ngowo et al.[65], was incorporated. It is therefore likely that both larval development time and adult mosquito size (either mass or wing length, which have been shown to be correlated[66]) are density dependent. The results with respect to larval mortality are more mixed, but it is possible that this is also density dependent.

These life-history characteristics are crucial to modelling mosquito population dynamics; development time and mortality need to be explicitly included in any model of *Anopheles*, and it has been observed that adult mosquito size impacts female fecundity[67], adult female survival[63], the growth rate of offspring, and male mating competitiveness[54] (all of which increase as adult size increases[54, 63, 64, 67]). Additionally, and crucially for models of malaria transmission, adult female size has also been found to affect both the number of blood-meals that a female mosquito seeks (smaller adult females will often seek multiple blood-meals before oviposition, not just one)[63, 67] and females' host seeking response (which decreases as size decreases)[63]. Both of these will in turn affect the local entomological inoculation rate (EIR, or the number of infectious bites a person receives per year), which drives the force of infection in many malaria models[36]. However, as discussed earlier, despite the experimental findings, the majority of models of gene drive dynamics in mosquito populations have assumed that only larval mortality is density-dependent, with the other two probable density-dependent characteristics ignored.

Aims and Objectives

Aim

To develop a mathematical model of *Anopheles gambiae s.l.* mosquito population dynamics that incorporates density-dependent variation in multiple mosquito demographic traits and to use the model to investigate how this affects predictions of the suppression effect of gene drives as a method for malaria control.

Objectives

- Develop a delay differential equation model for *Anopheles* mosquitoes that incorporates density-dependent larval development times and female fecundity, and parametrise this model to represent *Anopheles gambiae s.l.* mosquitoes.
- Determine the equilibrium solutions of the new model and analyse the stability of these solutions to better understand the model dynamics and behaviour. Perform a sensitivity analysis on a subset of parameter values that are important for malaria control interventions to examine how uncertainty in these parameter values impacts the model's predictions.
- Use the newly developed model to investigate the effects of a gene-drive release on adult mosquito suppression. Compare these effects with those predicted by other *Anopheles gambiae s.l.* models that assume density dependence acts only on larval mortality to assess how model structure and the assumptions made about density-dependence affect predictions of the efficacy of suppression gene drives.

Methods

The model developed in this project is an adaptation of an earlier model proposed by Nisbet and Gurney in their 1983 paper "The Systematic Formulation of Population Models for Insects with Dynamically Varying Instar Duration"[1]. Nisbet and Gurney formulated the model to represent the population dynamics of a damselfly[1], so to better capture the density-dependent dynamics of *Anopheles* mosquitoes, I modified the model to include an explicit pupal stage, with its own density-independent mortality and development time distribution, and the fecundity of adult female *Anopheles* mosquitoes was adjusted to be density-dependent, as suggested by the literature (see Introduction). Below, I briefly set out Nisbet and Gurney's model (diagram A, Figure 1) and its derivation (with the notation slightly adjusted for clarity) to better aid understanding of my modifications (diagram B, Figure 1).

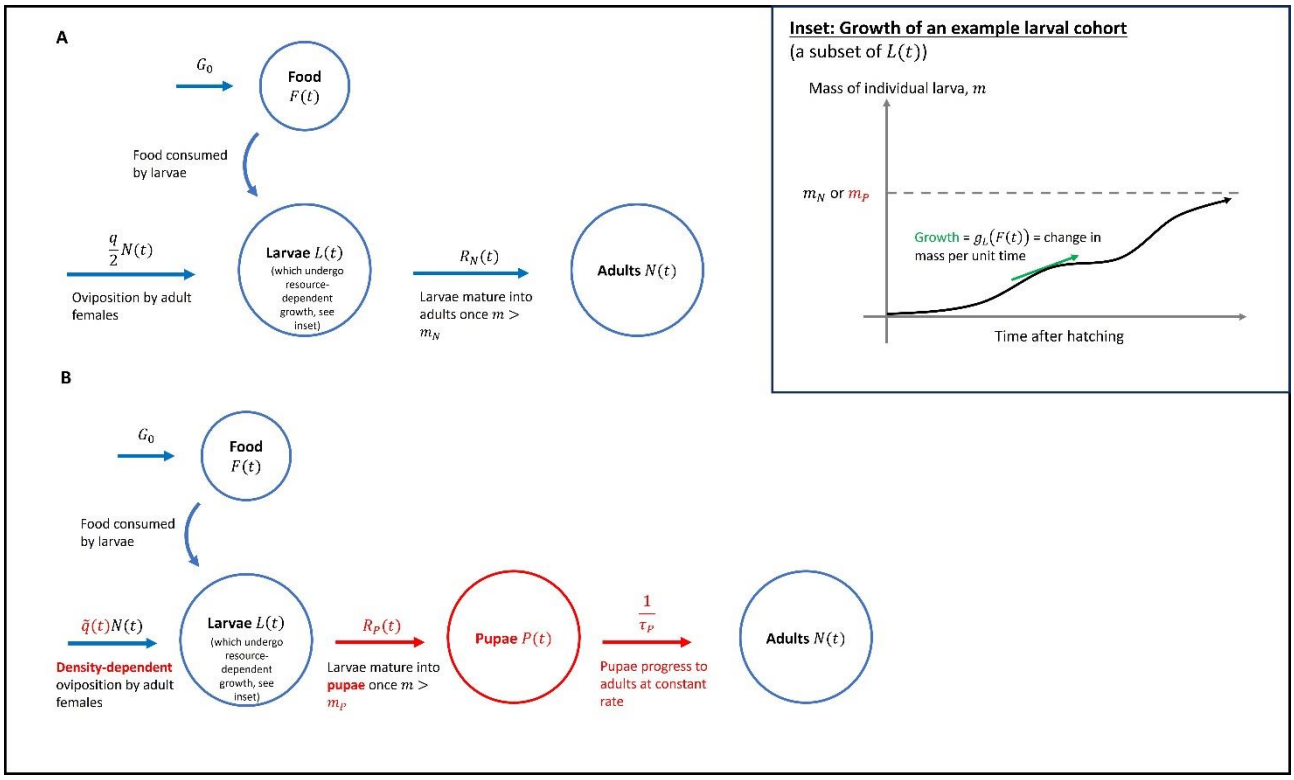

Figure 1: Diagrams showing the structure of Nisbet and Gurney's lumped age-class damselfly model (A, top) and the modified version of Nisbet and Gurney's model used in this project for Anopheles mosquitoes (B, bottom). Modifications to the original model are shown in red. The Inset in the top-right applies to both diagrams A and B, with red again indicating changes in model B from model A.

The Nisbet and Gurney Model

Nisbet and Gurney's "Strategic Model" for the damselfly is a specific case of a more general model for insect ecology based on lumped age classes, which the authors set out at the beginning of their paper. The basic idea underpinning this model is that the life cycle of an insect can be split into smaller sub-stages,

depending on the mass and developmental stage of the insect, and that all insects within a class can be considered to undergo demographic processes at the same rate. Nisbet and Gurney model the dynamics with a set of DDEs and split the life-cycle of a damselfly into two stages, with insects assumed to either be larvae, and therefore in class $L(t)$, or adults, and therefore in class $N(t)$[1]. Nisbet and Gurney assume that the time it takes larvae to develop into adults (i.e. the time they spend in the larval class $L(t)$) is density-dependent (see diagram A, Figure 1), but that mortality in both the larval and adult stages is density-independent, with this mortality occurring at constant per capita rates μ_L and μ_N respectively[1]. While these models are more complex to analyse than standard DDEs, where time delays are assumed to be fixed, analytic solutions for the equilibria can still be obtained (as shown below and in Supplementary Materials).

Adult female damselflies are assumed to have constant fecundity, meaning that larvae are born at a rate $\frac{q}{2}N(t)$, where q is the number of eggs that successfully hatch per female per day. Nisbet and Gurney then assume that larvae grow by consuming food from a food source $F(t)$ at rate $A_L(t)$ per larva. $A_L(t)$ is given by the equation:

$$A_L(t) = \frac{A_{max}F(t)}{K_F + F(t)} \tag{1}$$

where A_{max} is the maximum rate of food consumption per larva and K_F is a constant of proportionality that limits food consumption. Food is assumed to enter the habitat at a constant rate G_0, but before (and at) time $t = 0$ it is assumed that no food enters the habitat[1].

It is then assumed that the larval growth rate at time *t*, $g_L(t)$, is proportional to the rate that larvae consume food:

$$g_L(t) = \gamma A_L(t) \tag{2}$$

where γ is a constant of proportionality. This implies that the maximum rate of larval growth, g_{max}, is equal to γA_{max}[1].

A key assumption of the Nisbet and Gurney model is that there is a certain mass m_N at which larvae become adults, and that this mass is equal to the cumulative growth of the larvae from the time they hatch to the time they reach this mass (see diagram A, Figure 1). This relationship can be represented in the following equation:

$$m_N = \int_{t-\tau_L(t)}^{t} g_L(t')dt' \tag{3}$$

where $\tau_L(t)$ is the time taken for a larva to reach mass m_N. $\tau_L(t)$ is henceforth referred to as the larval development time.

Substituting equation (2) into equation (3) and then differentiating with respect to t (using the Leibniz rule for differentiation) yields the following delay differential equation for the larval development time $\tau_L(t)$[(1)]:

$$\frac{d\tau_L(t)}{dt} = 1 - \frac{F(t)\left(K_F + F\left(t-\tau_L(t)\right)\right)}{F\left(t-\tau_L(t)\right)\left(K_F + F(t)\right)} \tag{4}$$

Assuming that the amount of food in the habitat is constant up to and including time $t = 0$, i.e.:

$$F(t) = F_0 \; \forall \; t \leq 0 \tag{5}$$

gives us two further relationships. Firstly, combining equations (1)-(3) and (5) gives us an initial condition for $\tau_L(t)$:

$$m_N = \int_{t-\tau_L(t)}^{t} \frac{\gamma A_{max} F_0}{K_F + F_0} dt' = \frac{\gamma A_{max} F_0}{K_F + F_0}\tau_L(t) \; \forall \; t \leq 0 \tag{6}$$

$$\Rightarrow \tau_L(t) = \frac{m_N(K_F + F_0)}{\gamma A_{max} F_0} \; \forall \; t \leq 0 \tag{7}$$

Secondly, we can see from equations (1)-(3) that the shortest possible larval development time, $\tau_{L_{min}}$, occurs when the growth rate, $g_L(t)$, is at its maximum value, g_{max} for the entire larval development time period. This is only reached in the limit as $F(t) \to \infty$, but, using g_{max} as an upper bound for $g_L(t)$, we can bound $\tau_L(t)$ from below and write that:

$$m_N = g_{max}\tau_{L_{min}} = \gamma A_{max}\tau_{L_{min}} \tag{8}$$

The equation that represents the transition of damselflies from the larval class $L(t)$ into the adult class $N(t)$ is the most complicated part of Nisbet and Gurney's model. It can be thought of as the product of the density of larvae whose mass is just about to increase to the critical mass at which they become adults, and the growth rate of the larvae at that time[1]. This can be expressed mathematically as:

$$R_N(t) = \lim_{\epsilon \to 0^+} \rho(m_N - \epsilon, t) g_L(t) \tag{9}$$

where $R_N(t)$ is recruitment into the adult class and $\rho(m, t)$ is the density of damselflies of mass m at time t.

In Appendix 1 of their paper, Nisbet and Gurney provide a formula for $\rho(m_N, t)$ using a more general balance equation linking density, growth and death (see equation (5), p116 in their paper)[1]:

$$\rho(m_N, t) = \frac{R_L\big(t - \tau_L(t)\big)}{g_L\big(t - \tau_L(t)\big)} e^{-\mu_L \tau_L(t)} \tag{10}$$

i.e., the density of larvae/adults of mass m_N is equal to the density of larvae who were recruited to the larval class $\tau_L(t)$ days ago, $\frac{R_L(t-\tau_L(t))}{g_L(t-\tau_L(t))}$, where $R_L(t)$ is the recruitment to the larval class at time t, multiplied by the probability of those larvae surviving the larval development period of $\tau_L(t)$ days, $e^{-\mu_L \tau_L(t)}$.

Finally, Nisbet and Gurney assume that there are no larvae or adults in the system before (and at) time $t = 0$, and that the system is started by a constant introduction of eggs, $I_L(t) = J_1$, between time $t = 0$ and time T_1, where T_1 is small[1]. This gives the following system of DDEs, which fully characterises the system:

$$\frac{dF(t)}{dt} = G_0 - \frac{A_{max} L(t) F(t)}{K_F + F(t)} \tag{11}$$

$$\frac{dL(t)}{dt} = I_L(t) + \frac{qN(t)}{2} - \frac{qN\big(t - \tau_L(t)\big)}{2} e^{-\mu_L \tau_L(t)} \frac{F(t)\left(K_F + F\big(t - \tau_L(t)\big)\right)}{F\big(t - \tau_L(t)\big)\big(K_F + F(t)\big)} - \mu_L L(t) \tag{12}$$

$$\frac{dN(\mathrm{t})}{\mathrm{dt}} = \frac{qN\big(t-\tau_L(t)\big)}{2} e^{-\mu_L \tau_L(t)} \frac{F(t)\Big(K_F + F\big(t-\tau_L(t)\big)\Big)}{F\big(t-\tau_L(t)\big)\big(K_F + F(t)\big)} - \mu_N N(t) \tag{13}$$

$$\frac{d\tau_L(t)}{dt} = 1 - \frac{F(t)\Big(K_F + F\big(t-\tau_L(t)\big)\Big)}{F\big(t-\tau_L(t)\big)\big(K_F + F(t)\big)} \tag{14}$$

with initial conditions:

$$F(t) = F_0 \; \forall \; t \leq 0 \tag{15}$$

$$L(t) = 0 \; \forall \; t \leq 0 \tag{16}$$

$$N(t) = 0 \; \forall \; t \leq 0 \tag{17}$$

$$\tau_L(t) = \frac{m_N(K_F + F_0)}{\gamma A_{max} F_0} \; \forall \; t \leq 0 \tag{18}$$

The system has the following analytically-derivable equilibrium solution, which Nisbet and Gurney derive in Appendix 2 of their paper[1]. In the Supplementary Materials of this project, I derive the steady state of Nisbet and Gurney's model with an additional pupal class, which is similar to the derivation of the steady state of Nisbet and Gurney's original model. At the steady state we have that:

$$F* = \frac{K_F m_N \mu_L}{\gamma A_{max} \log\left(\frac{q}{2\mu_N}\right) - \; m_N \mu_L} \tag{19}$$

$$L* = \frac{G_0 \gamma \log\left(\frac{q}{2\mu_N}\right)}{m_N \mu_L} \tag{20}$$

$$N* = \frac{2G_0 \gamma \log\left(\frac{q}{2\mu_N}\right)}{m_N(\mathrm{q} - 2\mu_N)} \tag{21}$$

$$\tau_L* = \frac{1}{\mu_L} \log\left(\frac{q}{2\mu_N}\right) \tag{22}$$

where $F*$, $L*$, $N*$ and τ_L* are the equilibrium values of $F(t)$, $L(t)$, $N(t)$ and $\tau_L(t)$ respectively.

As Nisbet and Gurney write, this means that, for the steady state to be physical (i.e. none of the values of the states at equilibrium are negative), we must have both:

$$q > 2\mu_N \tag{23}$$

and

$$\gamma A_{max} \log\left(\frac{q}{2\mu_N}\right) > m_N \mu_L \tag{24}$$

Since m_N and μ_L are constant, positive parameters, the first of these conditions is necessary for the second. We therefore have that the second condition alone determines the physicality of the steady state (and, in fact, the stability of the steady state also, which is discussed more in Supplementary Materials).

Modifications to Nisbet and Gurney's model

Full model equations for a modified version of the Nisbet and Gurney model[1] tailored to represent *Anopheles* are presented in the Results section. The changes can be seen in diagram B of Figure 1, in which changes from the original Nisbet and Gurney model (diagram A) are highlighted in red. The methodology for developing the modified model is described below

Incorporating a Pupal Class

The model was modified in two ways, as mentioned above. Firstly, an explicit pupal class $P(t)$ was added to the model, with *Anopheles* now modelled as either larvae, pupae, or adults. This allowed the differing characteristics of the pupal and larval stages to be better represented, as juvenile *Anopheles* mosquitoes have increased mortality during the pupal stage[68-70], which could not be incorporated in Nisbet and Gurney's original model. Furthermore, *Anopheles* pupae do not feed[71] and are not affected by density dependent competition, so modelling them in the same way as larvae is unrealistic. In the updated model, *Anopheles* larvae progress to the pupal compartment upon reaching a critical mass m_P in exactly the same way as larvae progress to adults in Nisbet and Gurney's model formulation. It was also assumed that pupae

undergo constant density-independent mortality, and progress to the adult class at a constant rate of $\frac{1}{\tau_P}$, where τ_P is the average time spent as pupae by *Anopheles* mosquitoes.

Additionally, the system was modified to be initiated by the introduction of adult mosquitoes, $I_N(t)$ over the short time period T_1, rather than by the introduction of larvae, because the progression of larvae to pupae is modelled as depending on the population of adult mosquitoes $\tau_L(t)$ ago.

Incorporating Density-Dependent Fecundity

The second change was to incorporate density-dependent adult female *Anopheles* fecundity (see diagram B, Figure 1). As discussed in the Introduction, experimental studies have generally agreed that increased density experienced during larval development leads to decreased adult size, both in terms of mass and wing length[51, 53, 57, 58]. In turn, adult female wing length and mass are known to be associated with fecundity - the greater the mass/wing length, the greater the number of eggs laid[67]. This implies that fecundity is also density dependent, and should be modelled as such, in contrast to Nisbet and Gurney's original model. Based on the available experimental data, this was incorporated into Nisbet and Gurney's model by modifying the fecundity term q to depend on the larval development time experienced by the youngest adult mosquitoes, which at time t is $\tau_L(t - \tau_P)$ (as discussed below).

Larval development time was chosen for the relationship instead of larval density due to a paucity of experimental data on the relationship between fecundity and larval density. Experimental studies on larval density tend to use a limited number of density treatments in containers/habitats, the size of which depends on the author, so translating any relationship between larval density and adult fecundity from the literature to the model would be difficult. This is not an issue with the relationship between larval development time and fecundity, as there are experimentally derived relationships between larval development time and adult female size/wing length, and between adult female size/wing length and adult female fecundity. These relationships can be directly incorporated into the model, and the modelled development times should then mirror those seen experimentally. Calculating a complete age distribution of adult mosquitoes in the system and assigning their fecundity according to age-specific development

times would be difficult, so development time in the fecundity equation is approximated as the development time of the youngest adult mosquitoes at time t (those who entered the pupal stage at time $t - \tau_P$). This approximation was chosen because younger adult mosquitoes are more numerous than older adult mosquitoes, and, since development time is a function of larval density over the whole development period, this should not vary significantly among successive cohorts.

The formula for the average number of eggs hatched daily per adult mosquito, $\tilde{q}(t)$, was derived by considering experimental data. Gimnig et al.[57] found that the best fit to their data on larval development time and adult female mass (m_A) occurred with the following formula:

$$m_A = \frac{0.13\tau_L - 0.35}{\tau_L - 5} \tag{25}$$

Koella and Lyimo[66] provide the following relationship between adult female mass (m_A) and wing length (w_A):

$$m_A = 0.0037 w_A^{4.08} \tag{26}$$

Finally, Lyimo and Takken[67] found a linear relationship between adult female wing length and number of eggs laid (e_A):

$$e_A = \xi + \chi w_A \tag{27}$$

with the values of ξ and χ depending on whether adult females were collected as pupae and allowed to emerge into adults, blood feed, and oviposit, or whether indoor-resting blood-fed mosquitoes were collected and then allowed to oviposit. Since Lyimo and Takken[67] counted the number of eggs two days post-blood meal, the average of the two possible values for ξ and χ was divided by 3 (the length of *Anopheles*' gonotrophic cycle[2]) to give per day values. They were then scaled downwards to match White et al.'s[2] prior for the number of eggs laid per female mosquito (12.75) at their prior for the larval development period (10.84 days). This could be done as White et al.'s model also did not include an egg stage (see Introduction), so their prior takes failure to hatch into account[2]. Finally, these numbers were

divided by 2 to give the number per adult mosquito, not per adult female mosquito, and are denoted $\tilde{\xi}$ and $\tilde{\chi}$ below.

Combining equations (25)-(27) would give the following model for density dependent fecundity (per adult):

$$\tilde{q}(t) = \tilde{\xi} + \tilde{\chi}\left(\frac{0.13\tau_L(t-\tau_P) - 0.35}{0.0037(\tau_L(t-\tau_P) - 5)}\right)^{\frac{1}{4.08}} \quad (28)$$

This equation, however, has a discontinuity at $\tau_L(t - \tau_P) = 5$, so to avoid this possible issue we approximate the equation above with a combination of a linear and an exponential function, and let:

$$\tilde{q}(t) = \eta + \kappa e^{-\lambda(\tau_L(t-\tau_p)-5)} \quad (29)$$

where η, κ and λ are all constant, positive parameters, chosen to best approximate equation (28). We have also introduced $\tau_L(t-\tau_P) - 5$ into the power of the exponential relationship, instead of using $\tau_L(t-\tau_P)$. This is so that when $\tau_L(t-\tau_P) = 5$ days, the minimum experimentally seen development time[57], we have the same fecundity for any value of λ: $\tilde{q}(t) = \eta + \kappa$. I also experimented with a simpler representation of $\tilde{q}(t)$, which allowed greater analytic tractability but resulted in a more unstable system that less accurately represented experimental findings (see Supplementary Materials).

Parameterizing the model to represent *Anopheles gambiae* populations

A literature review of previous experimental and modelling studies was conducted to ascertain appropriate default parameter values (where possible) for *Anopheles gambiae sensu lato* mosquitoes. The default parameter values used, as well as descriptions of the parameter values and their units, are presented in Table 2 below. The parameters relating to density-dependent fecundity, κ, λ and η, were chosen to minimise the L2 norm of the difference between the experimentally-derived function (28) and its approximation, (29), between development times of 5.7 days (the shortest non-outlier development time from Gimnig et al.[57]) and 25 days (longest larval development time seen during the literature review of

experimental studies[56]). This meant that equation (29) provided a good approximation of equation (28) for reasonable larval development times.

Parameter	Description	Unit	Value	Source
$\mathbf{F_0}$	Initial mass of food	mg	20	Arbitrary, see above.
A_{max}	Maximum rate of food consumption per larvae	mg day^{-1}	0.3	Largest amount of food supplied per mosquito larva seen in experimental density-dependence studies[63], see above.
K_F	Constant of proportionality to relate food density and consumption	mg	10	To make initial food consumption per larva equal to 0.2mg day^{-1}, as per the most common experimentally used food treatment[48, 49, 54, 66], see above.
$\frac{m_p}{\gamma}$	Ratio of mass larvae become to pupae and the constant that relates maximum larval growth to maximum larval food consumption	mg	1.5	To make the minimum larval development time match that seen experimentally[57], see above.
G_0	Rate of food supply	mg day^{-1}	200	Arbitrary, see above.
T_1	Time over which larvae are inputted to start system	day	0.001	To make input equal to 100 adult mosquitoes, see above.
J_1	Rate of initial larval input	day^{-1}	100,000	To make input equal to 100 adult mosquitoes, see Methods.
μ_L	Per capita death rate of larvae	day^{-1}	0.248	Average from Service[68], Service[69] and Service[70].
μ_P	Per capita death rate of pupae	day^{-1}	0.395	Average from Service[68], Service[69] and Service[70].
μ_N	Per-capita death rate of adult mosquitoes	day^{-1}	0.091	Prior used by White et al.[2] (taken from Garki project (1980) .
τ_P	Average time spent as pupae	day	1	Prior used by White et al.[2] (actually Bayoh & Lindsay[61]).
κ	Fecundity-related parameter. κ is the number of eggs hatched per day per adult mosquito when the larval to pupal development time is 5 days, minus η.	day^{-1}	5.8	Chosen to best approximate equation (28), see above.
λ	Fecundity-related parameter. λ is the rate at which the number of eggs hatched per day per adult mosquito, minus η, decays for every day longer the adult's larval-to-pupal development time is.	day^{-1}	0.41	Chosen to best approximate equation (28), see above.
η	Fecundity-related parameter. η is the number of eggs hatched per day per adult mosquito in the limit as larval-to-pupal development time tends to infinity.	day^{-1}	5.6	Chosen to best approximate equation (28), see above.

Table 2: Summary of parameter values used.

For those parameters for which it was not possible to infer appropriate default values from the literature, such as the parameters J_1, T_1, F_0, A_{max}, $\mathrm{K_F}$ and G_0, values were assigned using the following rationale. It was arbitrarily decided that 100 adult mosquitoes should be inputted into the system, so to achieve this, J_1 was set to be 100,000 mosquitoes per day and T_1 0.001 days. It was also arbitrarily decided that F_0 should be set to 20mg. A_{max} was chosen as 0.3 mg/day, as this was the highest food-treatment given in the laboratory-based experimental studies reviewed[63], and K_F was then set to 10mg, as this would mean that:

$$A_L(0) = \frac{A_{max}F_0}{K_F + F_0} = 0.2 \ \ (mg\ day^{-1}) \tag{30}$$

i.e. the initial rate of food consumption per larva was the same as the amount of food per larva given to larvae most commonly in laboratory-based experimental studies on density-dependence[48, 49, 54, 66]. G_0 was set, arbitrarily, to be 200 mg day^{-1}, which would sustain a population of 1000 mosquito larvae if food was consumed at the initial rate.

The critical mass at which a larva completes development, m_P, and the scaling parameter γ always appear together, and always appear in the same ratio. The two parameters were therefore merged into the ratio $\frac{m_P}{\gamma}$, and this was set equal to 1.5, so that, with $A_{max} = 0.3$, we had that:

$$\tau_{L_{min}} = \frac{m_P}{\gamma A_{max}} = 5\ (days) \qquad (31)$$

which is equal to the shortest larval development time seen experimentally[57]. Equation (31) above is a rearrangement of equation (8) when a pupal class is included in the model.

Average adult female wing-length was calculated from the model's outputs using a combination of the experimentally-derived formulas (25) and (26). It was assumed that maximum wing length occurred with a larval development time of 5.7 days, the smallest non-outlier larval development time observed by Gimnig et al.[57], and that larval development times smaller than this also produced adult females with that maximum wing length. The probability of larval to pupal survival was calculated using the cumulative distribution function of the exponential distribution with rate parameter μ_L for the larval-to-pupal development time outputted by the model. Average fecundity was calculated using equation (29).

Coding

Model analyses were conducted in R version 4.3.2[72]. The model was coded and run using the odin: ODE generation and integration package (version 1.2.5)[73], which compiles models coded in R in C and includes the ability to numerically solve systems of DDEs. Other R packages used for analysis and data visualisation include: dplyr (version 1.1.3)[74], ggplot2 (version 3.4.4)[75], tidyverse (version 2.0.0)[76], MetBrewer (version 0.2.0)[77], scales (version 1.2.1)[78], ggthemes (version 4.2.4)[79], patchwork (version 1.1.3)[80] and rootSolve

(version 1.8.2.4)[81]. The code used in this project is available on GitHub and can be accessed with the following link: https://github.com/oliversimmons/MRes-Project-1

Sensitivity Analysis

Making the modifications to Nisbet and Gurney's[1] model detailed above, I developed a system of DDEs that fully characterised the system. As shown in Results, I derived an equilibrium solution for the model and verified, by simulating the model using the odin[73] package in R, that the long-term behaviour of the model matched this equilibrium solution. I then characterised the dynamics of the new model by numerically determining the stability of its steady state for varying model parameter values. The complex nature of the DDEs, however, meant that I was not able to perform an analytical stability analysis (as the addition of a time-varying delay, as opposed to a fixed delay, made the equations significantly more complicated to deal with).

The model exhibited both oscillatory behaviour and extinction for certain values of key parameters, so the following process was used to classify the behaviour exhibited by the model and to determine the long-term value of each state. For each set of parameter values, the model was run over 18250 days (50 years). If the final value of each state was within 0.00001 of all of the previous 1000 values of that state (so approximately constant for the previous 1000 days), the model was assumed to have reached a stable equilibrium, and the final value of each state was taken as the equilibrium value. Similarly, if the values of the larval, pupal, and adult states were all less than 0.00001 for the last 1000 days of the model run, it was assumed that the model had reached extinction, and again the final value of each state was taken as its long-term value. If neither of these conditions were satisfied, an algorithm was used to determine whether the model was slowly progressing to extinction or whether it was exhibiting oscillatory behaviour, and also to calculate the long-term value of the model's states in the oscillation scenario. This algorithm is detailed in the Supplementary Materials.

To characterise the model's behaviour over a range of key parameter values, I performed a series of local sensitivity analyses, varying certain key parameters individually over a range of values whilst keeping all other parameters at their default values. This allowed for the long-term behaviour of the model and the

long-term value of the model's states to be analysed. Particular attention was paid to the parameter values associated with fecundity (η, κ, and λ), as these were new parameters that had been introduced in the model update, as well as to the larval mortality parameter, μ_L, as it impacts the intensity of density dependence during the larval stage, and to the parameters relating to the carrying capacity of the model (G_0 and K_F). Following this, I performed further sensitivity analyses where multiple key parameters were varied at once, which allowed for an even wider range of the parameter space to be considered and enabled the interaction between the parameters to be seen more clearly.

Predicting the Impacts of Gene-drive Interventions

In a simple model of a gene drive, all individuals are designated as either wild-type, heterozygous for the modified gene or homozygous for the modified gene. If we assume that female mosquitoes homozygous for a modified suppression gene are completely sterile, but that there is no sterility effect on females heterozygous for the gene, then, if a suppression gene was homozygous in a proportion p_{GG} of the mosquito population, the average per capita fecundity of the population would decrease by a factor of $1 - p_{GG}$ i.e.

$$\hat{q}(t) = (1 - p_{GG})\tilde{q}(t) \; = \; (1 - p_{GG})\eta + (1 - p_{GG})\kappa e^{-\lambda(\tau_L(t-\tau_p)-5)} \qquad (32)$$

where $\hat{q}(t)$ is the average per capita daily fecundity after a suppression gene drive has been introduced.

This means that running the Modified Nisbet and Gurney model using $\hat{q}(t)$ instead of $\tilde{q}(t)$, which in practice is the same as multiplying both η and κ by $1 - p_{GG}$ (see above), is a simple way to simulate the effect of a suppression gene drive having become homozygous in a proportion p_{GG} of the population. The proportion of homozygous females reached in a population after the introduction of a gene drive may vary depending on a number of factors, including non-functional resistance, variance in the homing rate of the gene drive and potential fitness costs associated with the gene drive[28]. In my analysis I do not explicitly model these characteristics (see Discussion). Instead, to partially account for this, the equilibrium or long-term adult *Anopheles* population size was calculated for varying values of p_{GG} between 0 and 1.

Mosquitoes homozygous for a suppression gene have also been found to be unable to spread malaria due to anomalies in the proboscis[19]. Therefore, to work out the number of adult female mosquitoes able to spread malaria, half the long-term adult population for each value of p_{GG} was multiplied by the proportion of mosquitoes assumed to be not homozygous for the suppression gene, $1 - p_{GG}$ (assuming an even gender split), i.e.:

$$\widehat{N_F}(t) = (1 - p_{GG})N_F(t) = (1 - p_{GG})\frac{N(t)}{2}$$

where $N_F(t)$ is the number of adult female mosquitoes at time a t and $\widehat{N_F}(t)$ is the number of adult female mosquitoes at time t able to spread malaria after the introduction of a suppression gene drive.

Comparison with other Models of Larval Density-dependence

To investigate the effects that the density-dependence assumptions made in the new model would have on the impacts of a suppression gene drive, the changes in the long-term adult *Anopheles* population and the numbers of biting females were compared to those given by two other published *Anopheles* population dynamics models. These were White et al.'s ODE-based model[2] and Hancock and Godfray's fixed-delay DDE model[3]. Both of these models have been discussed in the Introduction section, but I will outline them again briefly here. Hancock and Godfray's model considers mosquitoes as either eggs, larvae, pupae or adults, and models development time as fixed between these life-stages[3]. Larval density-dependence manifests itself as a density-dependent daily larval mortality, and entry into and maturation from the larval stage is based on the lagged adult population, hence the use of DDEs. White et al.'s model has four stages, early-larval, late-larval, pupal and adult, with development times not fixed and progression to and from each compartment represented by ODEs[2]. White et al.'s model also assumes density-dependent daily larval mortality only[2]. Neither model considers density-dependent development time or fecundity.

A suppression gene drive was simulated in these two models in exactly the same way as in the Modified Nisbet and Gurney model; constant fecundity parameters (β in White et al.'s model[2] and λ in Hancock and Godfray's model[3]) were multiplied by $1 - p_{GG}$, where p_{GG} is the proportion of the population homozygous for the modified suppression gene. Importantly, both models have an analytical equilibrium solution that is

non-negative for most values of fecundity, so in the following comparison it is assumed that, if the analytical equilibrium solution is non-negative, the equilibrium solution is the long-term value of the adult population. If the analytical equilibrium solution is not non-negative, it is assumed that the adult population is extinct (which is a simplification as Hancock and Godfray's model did exhibit limit cycles in some areas of the parameter space[3]). Other parameters in the three models were taken as either their default values (in the case of Hancock and Godfray's model) or their posterior values (in the case of White et al.'s model). The parameters used are set out in Tables A1 and A2 in the Supplementary Materials. The only exception to this was that, to enable the model comparison to be made, the parameters relating to the carrying capacity of the mosquito habitat in the Hancock and Godfray model (the parameter γ_W) and in the modified Nisbet and Gurney model (G_0 (see Results)) were adjusted so that the equilibrium adult mosquito population of the three models at each model's default or posterior fecundity was the same. The reduction in the malaria-transmitting mosquito population was then calculated as above.

Uncertainty Analysis

To quantify the effects of parameter uncertainty on the impacts of a predicted suppression gene-drive, an uncertainty analysis was performed via Latin Hypercube Sampling (LHS) for each of the three models. The only parameters that were not varied were those relating to fecundity which are affected by the introduction of a suppression gene drive, and those relating to carrying capacity, which were kept constant at the values described above. Each parameter in each model was varied between 50% and 150% of its default values and this range was split into 100 intervals for each parameter. A random value was chosen for each of these intervals (assuming a Uniform distribution), resulting in 100 random values for each parameter that well-spanned the 50-150% range. These 100 random parameter values were then ordered randomly for each parameter, resulting in 100 sets of samples of the parameter space which satisfy LHS. p_{GG}, the factor by which the fecundity parameter in each model was reduced, was varied between 0 and 1 (to represent different proportions of the population becoming homozygous for a modified suppression gene), and the equilibrium (or long term) adult mosquito population was then calculated for each model for each p_{GG} for each of the 100 sets of LHS parameter values.

Results

A Modified Model representing Multiple Density-dependent Demographic Traits

I modified Nisbet and Gurney's original 1983 model[1] to incorporate an explicit pupal class and time-varying density-dependent adult female fecundity, complementing existing features such as density-dependent larval development time. Incorporating these additions into the original model equations ((11) – (14), see Methods) results in the following set of delay differential equations:

$$\frac{dF(t)}{dt} = G_0 - \frac{A_{max}L(t)F(t)}{K_F + F(t)} \tag{33}$$

$$\frac{dL(t)}{dt} = \tilde{q}(t)N(t) - \tilde{q}\big(t-\tau_L(t)\big)N\big(t-\tau_L(t)\big)e^{-\mu_L\tau_L(t)}\frac{F(t)\left(K_F + F\big(t-\tau_L(t)\big)\right)}{F\big(t-\tau_L(t)\big)\big(K_F+F(t)\big)} - \mu_L L(t) \tag{34}$$

$$\frac{\mathrm{dP(t)}}{\mathrm{dt}} = \tilde{q}\big(t-\tau_L(t)\big)N\big(t-\tau_L(t)\big)e^{-\mu_L\tau_L(t)}\frac{F(t)\left(K_F + F\big(t-\tau_L(t)\big)\right)}{F\big(t-\tau_L(t)\big)\big(K_F+F(t)\big)} - \frac{P(t)}{\tau_P} - \mu_P P(t) \tag{35}$$

$$\frac{dN(t)}{dt} = I_N(t) + \frac{P(t)}{\tau_P} - \mu_N N(t) \tag{36}$$

$$\frac{d\tau_L(t)}{dt} = 1 - \frac{F(t)\left(K_F + F\big(t-\tau_L(t)\big)\right)}{F\big(t-\tau_L(t)\big)\big(K_F+F(t)\big)} \tag{37}$$

with initial conditions:

$$F(t) = F_0 \;\forall\; t \le 0 \tag{38}$$

$$L(t) = 0 \;\forall\; t \le 0 \tag{39}$$

$$P(t) = 0 \;\forall\; t \le 0 \tag{40}$$

$$N(t) = 0 \;\forall\; t \le 0 \tag{41}$$

$$\tau_L(t) = \frac{m_p(K_F + F_0)}{\gamma A_{max} F_0} \;\forall\; t \le 0 \tag{42}$$

and where:

$$\tilde{q}(t) = \eta + \kappa e^{-\lambda(\tau_L(t-\tau_p)-5)} \tag{43}$$

where $F(t)$ is the density of food at time t, $L(t)$ the number of *Anopheles* larvae at time t, $P(t)$ the number of *Anopheles* pupae at time t, $N(t)$ the number of adult *Anopheles* mosquitoes at time t and $\tau_L(t)$ the larval-to-pupal development time of the larvae who became pupae at time t. The model parameters are defined in Table 2 in the Methods section. This new model is hereafter referred to as the "Modified Nisbet and Gurney model".

Unlike Nisbet and Gurney's original model, it is not possible to analytically derive a fully closed-form equilibrium solution for the new model. This is because we have, from equations (33)-(37), that, at equilibrium, $\tau_L *$ (the equilibrium larval-to-pupal development time) is the root of:

$$0 = \kappa e^{-(\lambda+ \mu_L)\tau_L* + 5\lambda} + \eta e^{-\mu_L\tau_L*} - \mu_N(1 + \tau_P\mu_P) \tag{44}$$

which is not analytically solvable. It is, however, possible to solve for $\tau_L *$ numerically and then write the equilibrium solutions of the other states in terms of $\tau_L *$. This would give us:

$$F *= \frac{K_F}{\frac{\gamma A_{max}\tau_L *}{m_P} - 1} \tag{45}$$

$$L * = \frac{\gamma G_0 \tau_L *}{m_P} \tag{46}$$

$$P * = \frac{\mu_L\mu_N\gamma G_0\tau_P\tau_L *}{m_P(\eta + \kappa e^{-\lambda(\tau_L* - 5)})(1 - e^{-\mu_L\tau_L*})} \tag{47}$$

$$N * = \frac{\mu_L\gamma G_0\tau_L *}{m_P(\eta + \kappa e^{-\lambda(\tau_L*-5)})(1 - e^{-\mu_L\tau_L*})} \tag{48}$$

$$\tau_L * = \tau_L * \tag{49}$$

where $F *$, $L *$, $P *$, $N *$ and $\tau_L *$ are the equilibrium values of $F(t)$, $L(t)$, $P(t)$, $N(t)$ and $\tau_L(t)$ respectively.

Equilibrium solutions (44) - (49) also enable us to infer certain important characteristics of the system. Since G_0 and K_F do not impact the value of $\tau_L *$ at equilibrium (equation (44)), it is possible to see the impact increasing or decreasing the values of these parameters will have on the system, using equations (45)-(49), assuming that the equilibrium solution is stable for all values of these parameters. If this were the case, increasing G_0 would increase the carrying capacity of the population, with higher numbers of larvae, pupae, and adults at equilibrium, without changing the equilibrium larval development time, female fecundity, or the amount of food in the system. Increasing K_F would increase the amount of food in the system at equilibrium, with all other states unchanged. It was confirmed numerically that, with other parameters set to their default values, varying either G_0 or K_F (separately) from 1% or 10% of their default values respectively to 10 times their default values does not change the qualitative stability of the steady state (it remains stable), and the model behaves as expected when varying these parameters (see Figure A1 in Supplementary materials). This means that G_0 can be used to vary the carrying capacity of the system.

Predicting the Population Dynamics of *Anopheles gambiae*

The equilibrium solution above (equations (44) - (49)) matches the equilibrium state reached by the model when it was simulated forward in time with the default parameters (as specified in Table 2, Methods) for 730 days (Figure 2, below). The value of every state fluctuates after the model is initialised before reaching equilibrium. After the model has reached equilibrium, the number of pupae in the habitat at any one time is small, 8.20 (plot B, Figure 2). The number of adult and larval mosquitoes are modelled to be much higher, 90.1 (plot C, Figure 2) and 2052.8 (plot A, Figure 2) respectively. Notably, in this scenario, the amount of food in the habitat is very low, 4.81 mg (see plot D, Figure 2), which implies that larvae eat the majority of the food supplied. The equilibrium larval development time of 15.4 days (plot E, Figure 2) is higher than that found experimentally[57], whereas the average adult female wing length (2.51 mm) (F, Figure 2) is within but on the low-side of the experimentally observed range[66, 67]. There are biases associated with both laboratory and field studies, which may account for this difference, but it should also be noted that the default parameter values used were estimates, and adjusting them may bring larval development time and wing length more in line with those values seen experimentally. The model's fecundity cannot be directly compared with experimental data, as it takes into account the probability of eggs hatching (not just the

number of eggs laid), but at 5.79 (plot G, Figure 2), it is slightly lower than the prior used by White et al[2], who define fecundity in a similar way.

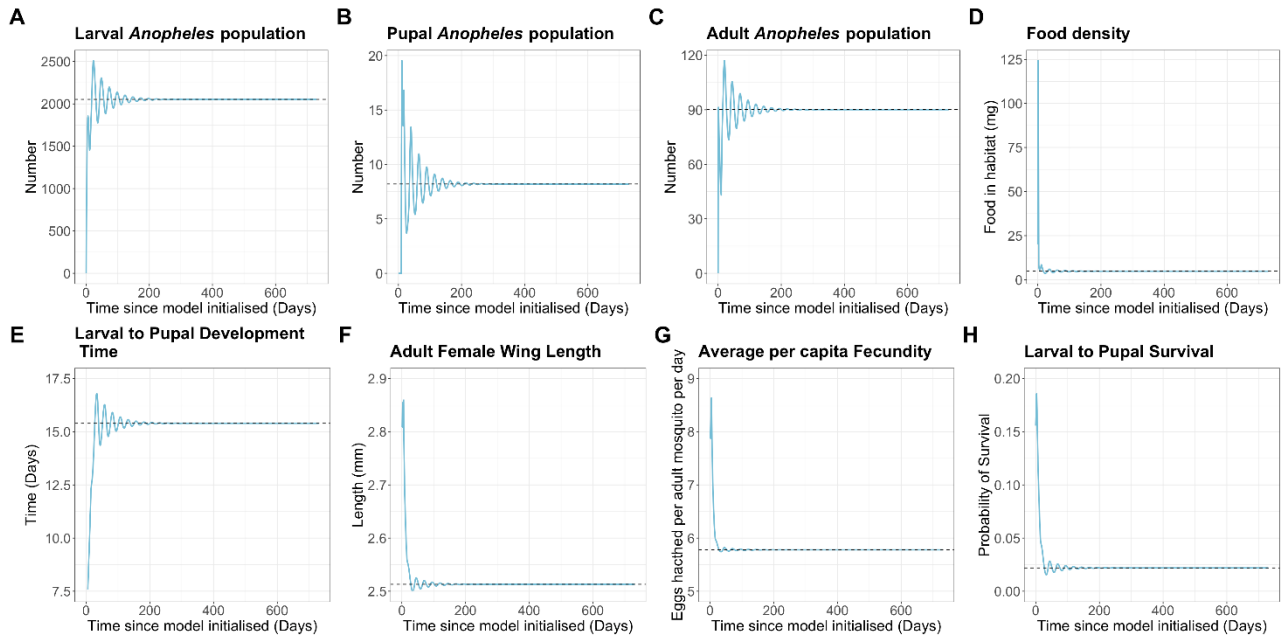

Figure 2: Output of the Modified Nisbet and Gurney model over 2 years when run with default parameter values. Blue lines indicate the value of the model's states over the 2 years. Dashed black horizontal lines indicate the equilibrium solution calculated using the model equations above.

Sensitivity to Female Fecundity and Larval Mortality Parameters

Local sensitivity analyses of certain parameters were conducted to ascertain at what values the long-term behaviour of the model qualitatively changes, assuming all other parameters remain at their default values. Parameters of particular interest were η, κ and λ, the new parameters introduced when time varying fecundity was added to the original Nisbet and Gurney model[1]. λ controls the extent to which fecundity is density dependent (for example $\lambda = 0$ would mean no density-dependence) and $\eta + \kappa$ is the average per capita fecundity of adults who experienced larval to pupal development times of 5 days. This is the minimum development time possible with the default parameter values used (see Methods), so, since $\tilde{q}(t)$ is monotonically decreasing with larval development time, $\eta + \kappa$ is the maximum per capita daily fecundity that can be seen. In the following analysis, the value of $\eta + \kappa$ was varied, rather than varying η or κ individually, because a reduction in female fecundity of $x\%$ would, in this model, be the same as reducing $\eta + \kappa$ by $x\%$. It is also valuable to understand the impact of varying larval mortality (μ_L), as this parameter effectively controls the intensity of density dependence (lower μ_L means fewer larvae dying, which in turn

means density dependence plays a larger role in reducing the larval population size) and is highly variable in field populations[82].

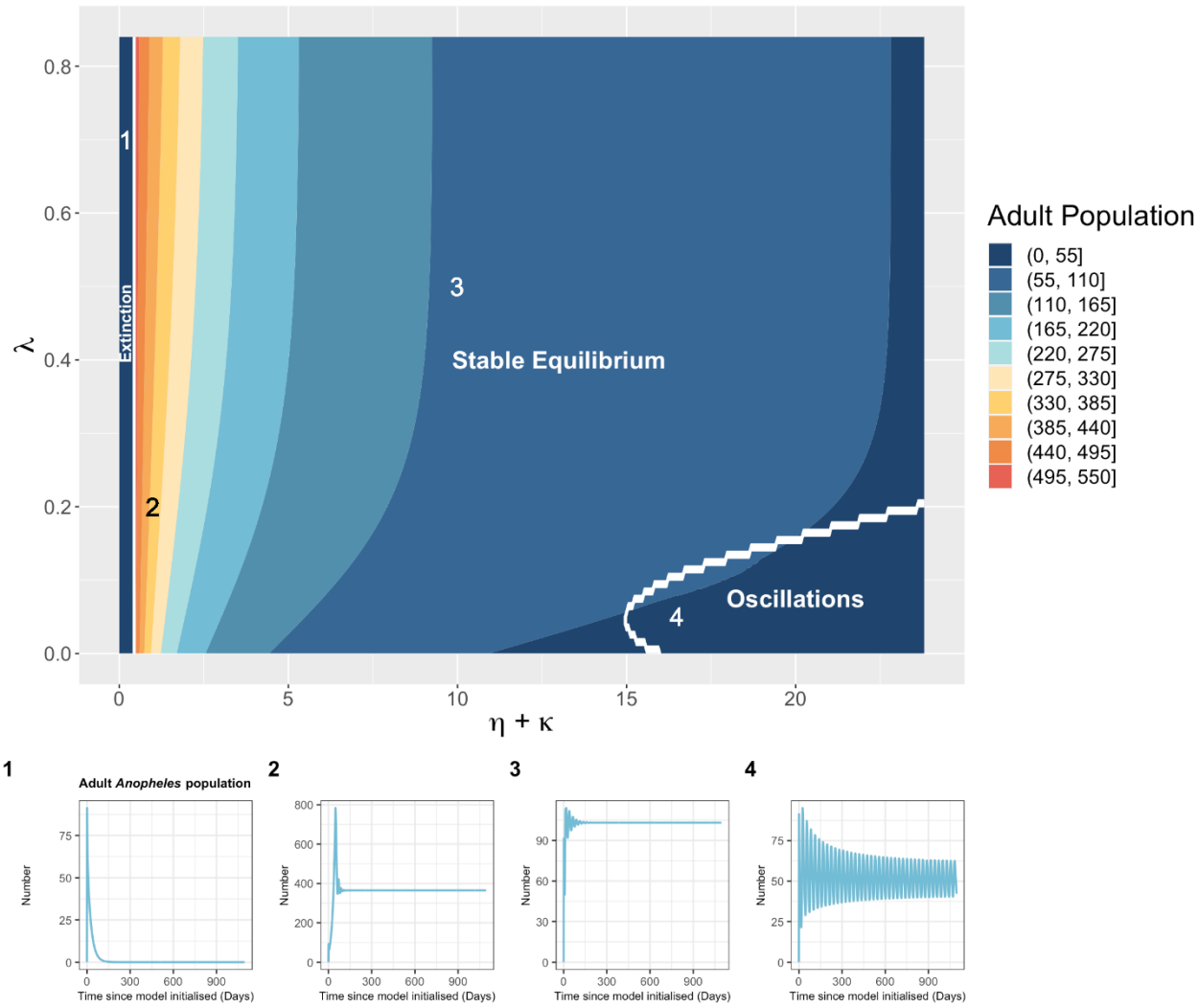

Figure 3: Top: Contour plot of the average long-term adult mosquito population size for varying λ and $\eta + \kappa$, where population size increases as the colour changes from dark blue to dark red, as per the key. $\eta + \kappa$ is the average per capita fecundity when adults experienced a larval-to-pupal development time of 5 days, and, as parameterised, is the maximum possible fecundity in the model. λ controls the extent of the fecundity's density-dependence ($\lambda = 0$ means no density dependence). The default values of λ and $\eta + \kappa$ corresponds to the mid-point of both axes, as both have been varied between 0 and 2 times their original values. White lines indicate the points at which the qualitative long-term behaviour of the adult population changes, and these regions are labelled in white. Bottom: Plots showing the fluctuation in the average adult population size over 3 years post-initialisation for 4 different sets of parameter values, where the values of λ and $\eta + \kappa$ used are indicated on the contour plot above by the number assigned to each plot.

We first consider a parameter space where λ varies together with $\eta + \kappa$. Across the majority of the parameter space, including at the default values of η, κ and λ, the model produces a stable equilibrium of varying adult population size (Figure 3, above, and plots 2 and 3, Figure 3). Not all areas of the parameter space result in a stable equilibrium, however, with the model exhibiting both oscillatory behaviour (where no equilibrium state is reached but instead the solution oscillates between fixed values, see Figure 3, plot 4), and population extinction (where all pupae, larvae and adult mosquitoes die out, see Figure 3, plot 1).

The density-dependent fecundity parameter λ has limited impact on adult population size, except at higher values $\eta + \kappa$ (Figure 3), whereas decreasing $\eta + \kappa$ (which is equivalent to decreasing the maximum average fecundity mosquitoes can experience) always increases long-term adult population size, implying overcompensation. This, however, only happens up to a certain value of $\eta + \kappa$, at which point the adult population becomes extinct. This occurs at $\eta + \kappa$ equal to 3.7% of their original values, i.e. an average per capita fecundity of 0.44 when the larval to pupal development time is 5 days. This extinction threshold is independent of λ, and thus the model does not predict any undercompensatory behaviour leading up to the threshold (Figure 3). At high values of $\eta + \kappa$ and at low values of λ, the adult population moves from a stable equilibrium to experiencing oscillations of varying periods (see plot 4, Figure 3). Interestingly, this seems to coincide with the lowest average long-term adult population sizes seen.

When μ_L is varied together with $\eta + \kappa$, all qualitative long-term behaviour of the model is possible (stable equilibrium, extinction, and oscillations), and again stable equilibrium is the most common behaviour (including at default values, see Figure 4, below, and plots 6 and 7, Figure 4). However, in this contour plot, the space in which oscillatory behaviour occurs is much larger. Again, adult population size always increases as $\eta + \kappa$ decreases (demonstrating overcompensation), but the amount by which it can increase is determined by the size of μ_L, with the highest average population sizes occurring with low $\eta + \kappa$ and low μ_L. Additionally, the highest average population size seen here is much higher than in Figure 3 (520.9 vs 1036 adult mosquitoes), although it should be noted that the magnitude of these values is determined by other factors, such as the carrying capacity of the model (discussed above). Decreasing $\eta + \kappa$ has a larger effect on population sizes at lower values of μ_L, and decreasing μ_L also has a larger effect at smaller values of $\eta + \kappa$.

The adult mosquito population becomes extinct for certain values of μ_L and $\eta + \kappa$, and the highest possible adult population size for each value of μ_L occurs immediately before the extinction threshold of $\eta + \kappa$ (as when λ was varied instead of μ_L), after which the population becomes extinct (Figure 4). Unlike λ, μ_L also has an effect on the extinction threshold of the model, with extinction at larger values of $\eta + \kappa$ for higher

values of μ_L. Oscillations occurred over a wide range of values of $\eta + \kappa$ and at lower values of μ_L, with the latter parameter seeming to have a greater impact on the model's stability.

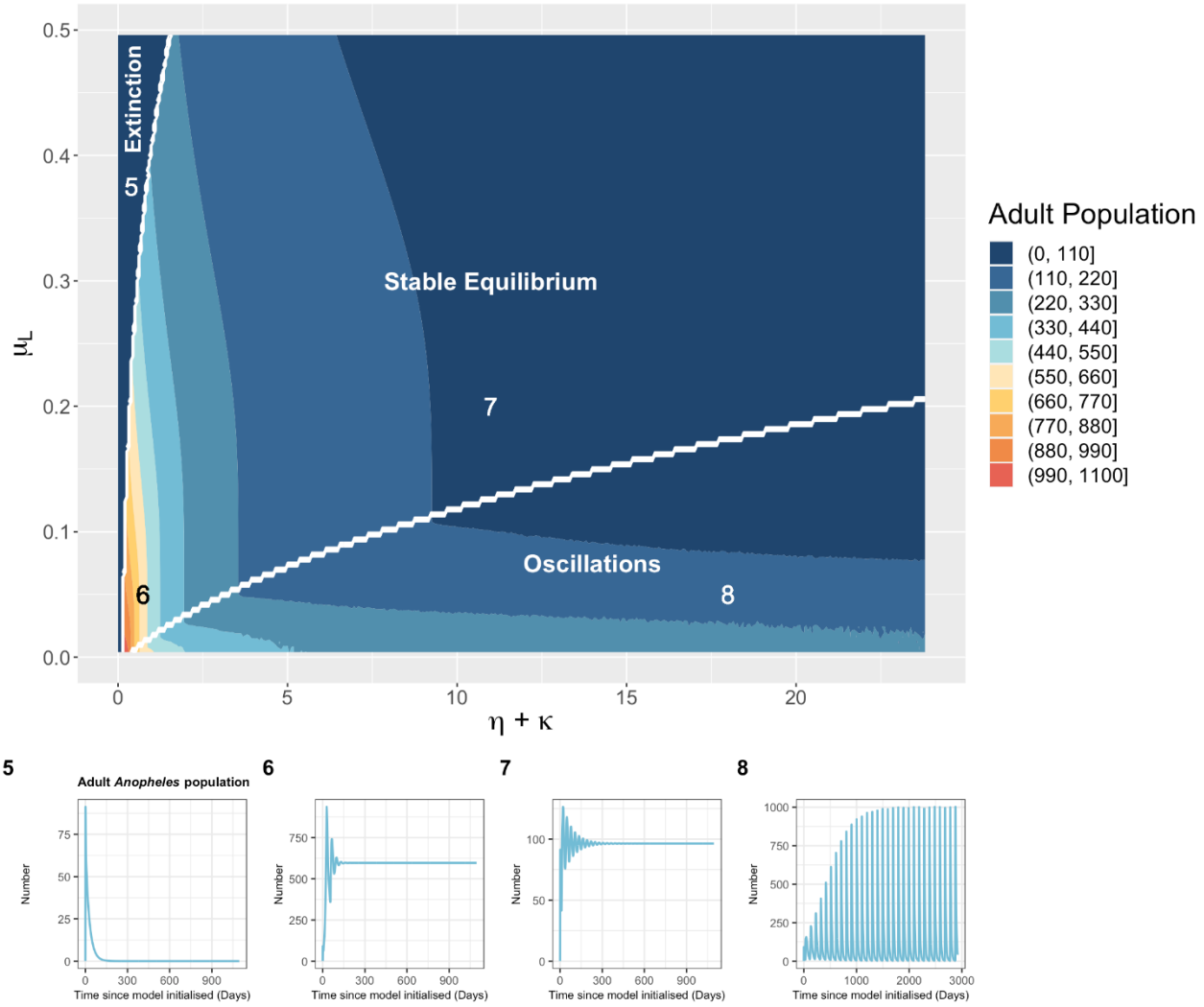

Figure 4: Top: Contour plot of the average long-term adult mosquito population size for varying μ_L (y-axis) and $\eta + \kappa$ (x-axis), where population size increases as the colour changes from dark blue to dark red, as per the key. The default values of μ_L and $\eta + \kappa$ correspond to the mid-point of both axes, as they have both been varied between 0 and 2 times their original values. White lines indicate the points at which the qualitative long-term behaviour of the adult population changes, and these regions are labelled in white. All other parameters are kept at their default values.
Bottom: Plots showing the fluctuation in the average adult population size over 3 years post-introduction (plots 1-3) or 8 years post-introduction (plot 4) for 4 different sets of parameter values, where the values of μ_L and $\eta + \kappa$ used are indicated on the contour plot above by the number assigned to each plot.

Effects of Density-independent Larval Mortality on Density-dependent Demographic Traits

Changing the value of μ_L alters the intensity of larval density-dependent competition, impacting the density-dependent demographic traits modelled: larval-to-pupal development time and per capita fecundity. Varying μ_L from between 0.1 and 0.496 (an upper limit of double the default value and a lower limit that does not result in extreme larval development times) whilst keeping all other parameters at their default

values shows that, as μ_L increases, larval-to-pupal development time decreases (Figure 5A), and per capita fecundity increases (Figure 5B). This means that if larval competition increases, due to larval mortality decreasing and therefore more larvae surviving every day, larval development time increases and fecundity decreases. The model is therefore behaving as expected, with density dependence occurring in the manner suggested by experimental studies.

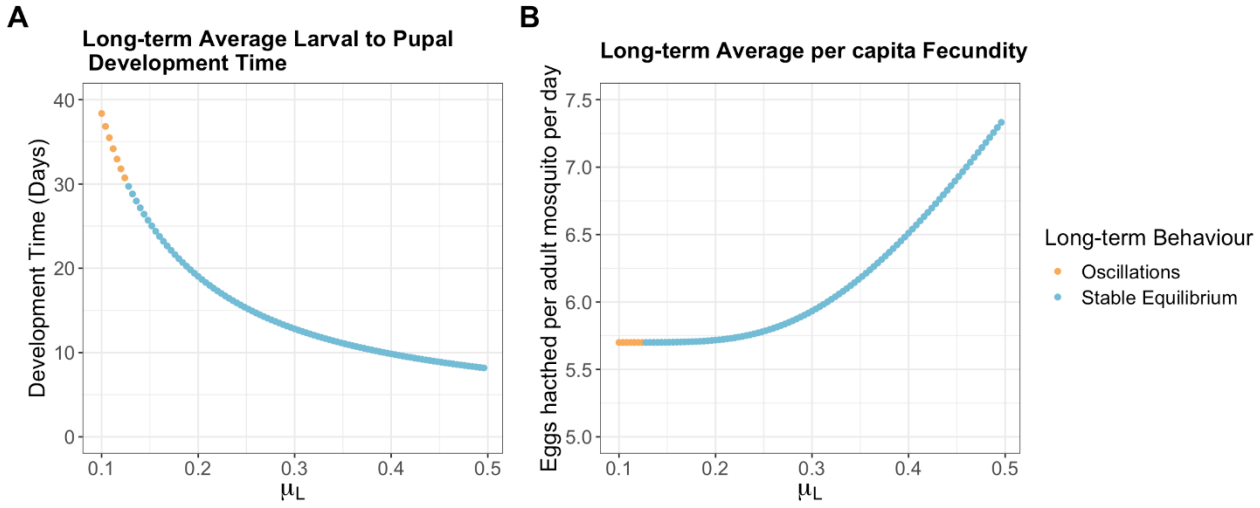

Figure 5: The impact of changing μ_L on long-term average larval-to-pupal development time (plot A, left) and on average per capita fecundity (plot B, right), both of which are density dependent. Each point represents a model run. Blue points indicate that the adult population reached a stable equilibrium and orange points that the adult population experienced oscillatory behaviour.

Predicting the Impacts of a Suppression Gene Drive

The effects of the introduction of a suppression gene drive are modelled by assuming that it would reduce the average fecundity of females by a factor of $1 - p_{GG}$, where p_{GG} is the proportion of the population homozygous for the gene drive (see Methods). Increasing the proportion of the population homozygous for the modified suppression gene from 0 to 1 in the Modified Nisbet and Gurney model causes the equilibrium number of adult mosquitoes in the population to increase (plot A, Figure 6). The number of adults in the population increases until the average per capita fecundity reaches an extinction threshold (approximately 96% of the population homozygous when default parameter values are used with an adjusted carrying capacity, see Methods), at which point the equilibrium number of adults in the population becomes zero. The uncertainty intervals generated from Latin Hypercube Sampling are wide, but the trend of increasing adult population size with decreasing fecundity occurred for all LHS parameter sets except one, for which the adult population was extinct for all values of fecundity (see Figure A2, Supplementary Materials).

In contrast, a gene drive becoming homozygous in a larger proportion of the population in the Modified Nisbet and Gurney model results in the equilibrium larval population decreasing (again until the extinction threshold is reached, see plot D, Figure 6). This suggests that, despite the larval population decreasing, the adult mosquito population overcompensates after the introduction of a gene-drive.

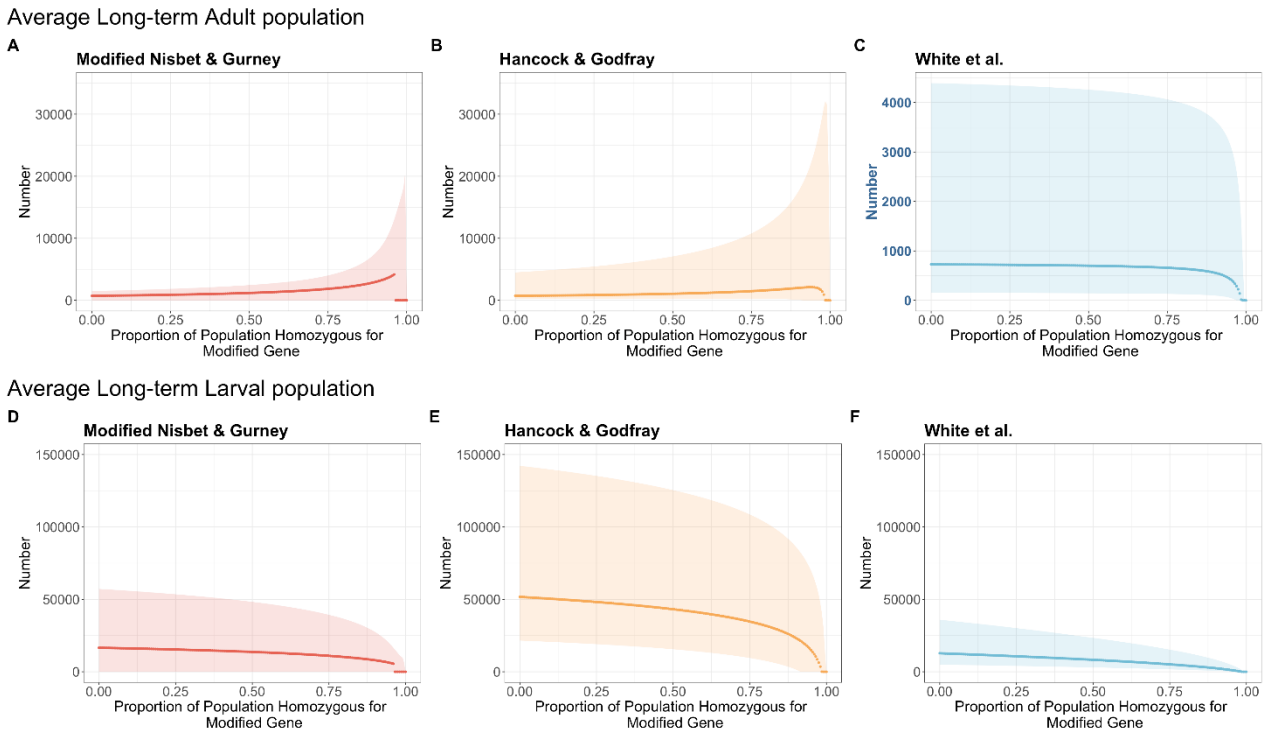

Figure 6: Comparison of the long-term or equilibrium adult (top row) and larval (bottom row) populations of the Modified Nisbet and Gurney model (leftmost column, plots A and D), the Hancock and Godfray model (2007) (middle column, plots B and E) and the White et al. model (2011) (rightmost column, plots C and F) when a suppression gene drive becomes homozygous in a fixed proportion of the adult mosquito population between 0 and 1. Here the solid line is generated by using each model's default or posterior values for every parameter except fecundity and a carrying capacity-related parameter (see Methods), and the shaded region is the range of results generated by considering model parameter uncertainty using Latin Hypercube Sampling (see Methods). The blue y-axis labels on plot C indicate that it has a different range to plots A & B, which both have the same y-axis range. Plots D, E & F all have the same y-axis range.

To investigate whether these behaviours were consistent across other widely used models of mosquito population dynamics, I compared the long-term behaviour of the adult population in the modified Nisbet and Gurney model to the equilibrium solutions of White et al.'s[2] and Hancock and Godfray's[3] models, as described in Methods. Increasing the proportion of the population homozygous for the modified gene has a similar effect on Hancock and Godfray's model as it has on the Modified Nisbet and Gurney model; decreasing adult fecundity causes overcompensation, causing the adult population to increase (plot B, Figure 6). The uncertainty intervals were again relatively large for the Hancock and Godfray model, but the model showed the same overcompensatory behaviour for each set of LHS parameter values (Figure A2,

Supplementary Materials). Both of these models use a DDE structure, but it is notable that this behavioural similarity occurs despite the density-dependent assumptions of the two models differing greatly - the Modified Nisbet and Gurney model assumes larval development time and adult female fecundity are density-dependent, while the Hancock and Godfray model assumes that only the daily larval mortality is density-dependent.

In contrast, White et al.'s model predicts that the adult population undercompensates as fecundity decreases, decreasing until the population becomes extinct at a low value of female fecundity (plot C, Figure 6). Additionally, no matter the set of parameters used, the same undercompensatory trend can be seen (Figure A2, Supplementary Materials). This behavioural difference seems to occur despite the fact that all three models predict decreases in the larval population abundance when adult female fecundity decreases (bottom row (plots D, E and F), Figure 6). The difference in the behaviour of White et al.'s model compared to that of the other two models could possibly be attributed to the differences in the way larval development is modelled. In White et al.'s ODE model, larvae accumulate less as fecundity increases, as any increase in the larval population instantaneously causes more larvae to transition out of the larval compartments. This then results in less intense density-dependent competition amongst the larvae, and undercompensation. In contrast, in the two DDE-based models, any increase in the larval population takes the length of the larval development time to impact the number of larvae maturing, allowing larger larval populations to accumulate as fecundity increases. This in turn increases density dependent larval competition and causes overcompensation.

The qualitative behaviours of the Modified Nisbet and Gurney model and the Hancock and Godfray model do, however, diverge as the extinction threshold of each model is approached. Increasing the proportion of the population homozygous for the modified gene in the Modified Nisbet and Gurney model causes the adult population to increase to its maximum value just before the extinction threshold, at which point it immediately becomes extinct (plot A, Figure 6). In Hancock and Godfray's model, however, as the proportion homozygous for the modified gene approaches the extinction threshold, the adult mosquito population experiences undercompensation, with the population decreasing rapidly to 0 (plot B, Figure 6).

Despite the overcompensatory behaviour of both the Hancock & Godfray model and the Modified Nisbet & Gurney model, all three models predict that the proportion of the original female *An. gambiae s.l.* population able to spread malaria would decrease as the equilibrium proportion of the population homozygous for the modified gene increases (Figure 7, plot A (below)). However, due to the differences in overcompensation and undercompensation seen amongst the three models, the predictions of the efficacy of such a gene drive vary. This difference is greatest when the gene drive has become homozygous in 74% of the mosquito population, at which point White et al.'s model predicted that the number of adult female *An. gambiae s.l.* mosquitoes able to spread malaria would decrease by 76.4%. Compare this to Hancock and Godfray's model, which would suggest a reduction of 47.8% and the Modified Nisbet and Gurney model, which would suggest a reduction of only 35.3% (plot A, Figure 7). Nevertheless, the models' predictions of the impact of a suppression gene drive converge again as the proportion of the population homozygous for the modified gene increases towards 1, becoming identical once the extinction thresholds of all three models have been reached.

White et al.'s model predicts the largest effect from a potential gene drive, as the adult population, in addition to becoming increasingly unable to spread malaria, undercompensates as the gene drive becomes homozygous in a larger proportion of the population. The Modified Nisbet and Gurney model developed in this paper in turn is more pessimistic about the impact of a potential gene drive, as it predicts the greatest overcompensation in the adult population when fecundity is decreased. Interestingly, the Modified Nisbet and Gurney model suggests that the introduction of a suppression gene drive would cause larval development time to decrease due to the reduction in density-dependent larval competition caused by the decreased larval population (plot B, Figure 7). This in turn means that the average wing length, and therefore size, of the adult female mosquito population increases from 2.51 mm to a maximum of 3.42 mm just before the extinction threshold is reached (plot B, Figure 7).

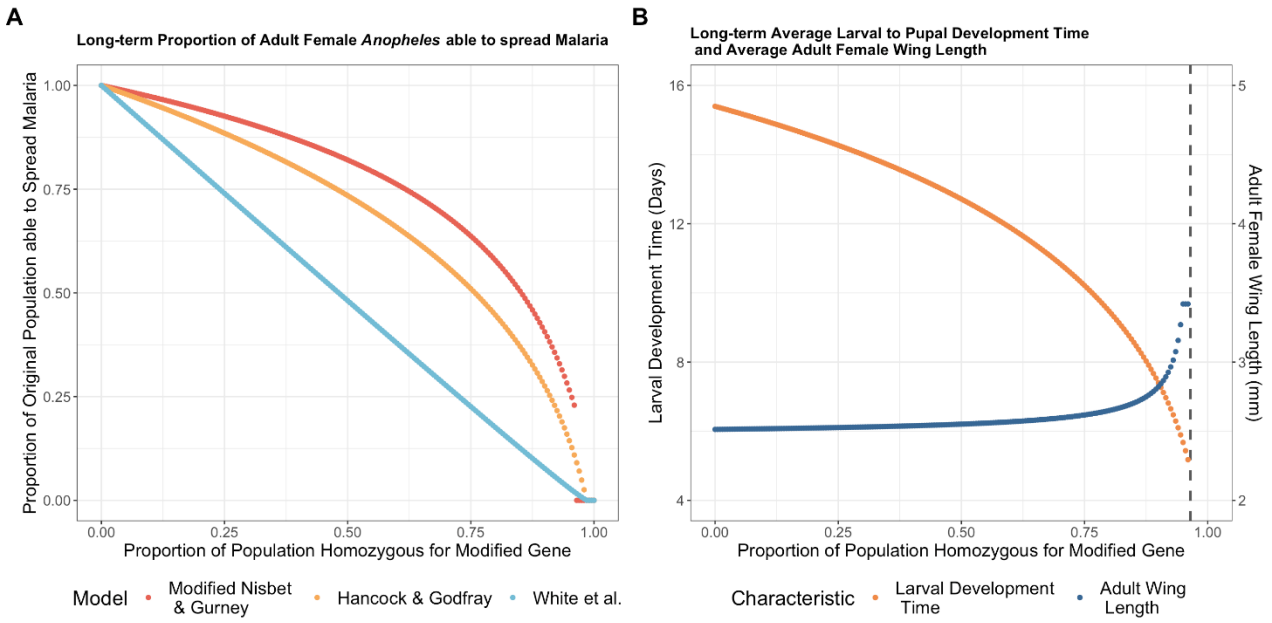

Figure 7: Plot A, left: Impact of a potential suppression gene drive that confers both infertility and an inability to spread malaria when it is homozygous in a female Anopheles mosquito across three different models: the Modified Nisbet and Gurney model (red), the Hancock and Godfray model (orange) and the White et al. model (light blue).. Here all model parameters are at their default or posterior values except fecundity and a carrying-capacity related parameter (see Methods).
Plot B, right: Change in long-term larval-to-pupal development time (orange) and average adult female wing length (dark blue) for different proportions of the mosquito population homozygous for a modified suppression gene, using the Modified Nisbet and Gurney model. The dashed line in the right-most plot indicates the extinction threshold, beyond which development time and wing length do not make sense.

Discussion

In this project I created a mathematical model for *Anopheles gambiae s.l.* mosquitoes that takes into account certain key experimentally-established density-dependent processes, expanding on the work of Nisbet and Gurney in the 1980s. The modelling work done in this project suggests that the introduction of a suppression gene drive into an *An. gambiae s.l.* population would be less effective at reducing the number of mosquitoes able to spread malaria than would be predicted other widely used models of mosquito population dynamics. The newly-developed model predicts that the number of adult *An. gambiae s.l.* females able to spread malaria will decrease after the introduction of a suppression gene drive, but that the size of the adult *An. gambiae s.l.* population will increase. This is due to the substantial overcompensation demonstrated by the adult *Anopheles* population when the average per capita fecundity of adults is decreased, as would occur with a suppression gene-drive. Hancock and Godfray's[3] model also shows significant overcompensation when fecundity is reduced, at least until fecundity becomes very small. However, despite these similarities, the new model predicted that a gene-drive that would be less effective than Hancock and Godfray's model.

White et al.'s[2] model, in contrast to the other two models, predicts that the adult mosquito population would decrease if the average fecundity was to decrease. This means that the impact of a suppression gene drive on malaria transmission when White et al.'s model is used is much greater than when the model developed in this project (or Hancock and Godfray's model) is used. However, it is notable, firstly, that the predictions of the three models studied converge as fecundity decreases to low levels, despite the new model predicting that the adult *Anopheles* population will be at its largest levels immediately before the extinction fecundity-threshold. Secondly, since all three models contain values of fecundity at which the adult *Anopheles* population becomes extinct, all three models predict that a suppression gene-drive, if spread to a high enough proportion of the *An. gambiae s.l.* population, would eliminate malaria transmission amongst that species of mosquito. Finally, and significantly, all three models, regardless of their varying assumptions about *An. gambiae* larvae's density-dependence, suggest that a suppression

gene-drive would decrease malaria transmission, no matter the percentage of the population that is homozygous for the modified suppression gene.

With this new model structure, decreasing the fecundity of adult females decreases the time *Anopheles* larvae take to develop, reducing the intensity of density dependence and resulting in larger adult mosquitoes. Questions remain over how a physically larger adult female *An. gambiae* population would affect malaria transmission. Larger adults need to bite less often for survival at the start of adulthood[63], which could reduce malaria transmission. However, larger adults also have increased survivorship and an increased host-seeking response when compared to smaller adults, which could increase transmission[63]. Furthermore, the environmental impacts of a physically larger, more numerous (but not malaria-transmitting) *An. gambiae s.l.* population, which the newly developed Modified Nisbet and Gurney model predicts, should be taken into consideration before gene-drives are introduced in the field.

The analysis conducted above does not consider all the density dependent factors that may impact wild *Anopheles* populations, such as Allee effects[83], predation of larvae by other species, and the cannibalism of younger larvae by older larvae[84]. Climatic factors such as temperature have also been found to significantly affect both larval mortality and development time[61, 85], and were not considered here. Nevertheless, Russell et al.[64] found that their field data supported a model for population growth that included density dependence based on a habitat carrying capacity, and that the growth rate of the *An. gambiae s.l.* population was associated with maternal wing length, with greater maternal wing at lower population densities. These findings motivate the representation of density dependence adopted here.

A major limitation of the project was the way the introduction of a gene drive was modelled. As mentioned in the Methods section, the way suppression gene drives were modelled did not explicitly consider any fitness costs for mosquitos heterozygous for the modified gene (e.g. via heterozygous mosquitoes having reduced fecundity when compared to wild type mosquitoes[19]), which would impact its spread through the population[20, 28]. The homing rate of the modified gene was also not explicitly modelled, which again would impact its spread, with higher homing resulting in greater suppression of the numbers of biting females[28]. Furthermore, the development of any functional or non-functional resistance to the gene drive, which is

crucial to understanding its efficacy, was not explored in this project[20, 28]. Instead, to partially account for these factors, the suppression effects of a range of possible equilibrium proportions of the population homozygous for the gene drive were simulated. This, however, gave no indication of what equilibrium proportion of the population homozygous would be expected for a suppression gene drive, and meant that I was unable to ascertain the effects of the modelled density-dependent demographic characteristics on the way the gene drive would spread through a population, limiting the insights that could be gained on the process.

Anopheles mosquitoes take an estimated 2-3 days to hatch[71, 86], during which time they experience a different daily mortality to at any other stage. To make the model as parsimonious as possible, this aspect of a mosquito's life cycle was not included in the final version. The model therefore makes the assumption, via a reduced fecundity term that accounts for this survival, that adult mosquitoes give birth to live larvae, but not including this lag between oviposition and hatching may make the model's results less accurate. Additionally, larval mortality may vary depending on whether the larva is in its first, second, third or fourth instar[68, 70]. If this is the case, this is not fully captured in the model, as it is assumed that all larvae have a fixed daily mortality, unaffected by their age. Mortality is also unaffected by the density of larvae in the system. This choice was again made for parsimony, as density-dependent mortality was the least experimentally supported density-dependent characteristic. Nevertheless, many papers do suggest that density-dependence is a factor, and although the model does account for larval-to-pupal survivorship decreasing as larval density increases by way of longer larval development times, density-dependent mortality may not be fully captured in the model.

Experimental studies have also found that adult survivorship decreases as adult size decreases[63]. Since the average adult size in the model is captured with an auxiliary equation based on larval development time (see Methods) taken from Gimnig et al.[57], the model does not take into account any effect on survivorship from changes in average size, with the daily adult mortality term μ_N constant in time. This means that, despite their lower fecundity, adults who experienced longer development times as larvae will, on average,

lay more eggs over their lifetime than they should (as their lifespan will be longer than it should be). This could motivate the addition of density-dependent adult mortality in future versions of the model.

The model for density dependent fecundity was taken from a series of best-fit relationships from experimental studies, and subsequently these best-fit relationships only had to deal with the values of larval development time, adult size and adult wing length that were seen experimentally. As a consequence, the density-dependent fecundity relationship used approaches a lower limit as larval development time tends to infinity, namely η. This is a reasonable approximation if larval development times are not too large but means that there is little difference between the fecundity of a female mosquito with a development time of 20 days and 100 days; a clearly problematic relationship as, even if they could exist, any mosquito with such a long larval development time would be so small as to not produce any eggs.

The design of the model, delay differential equations with time-varying delays, meant that it was not possible to conduct a stability analysis of the steady state of the model, which would have enabled extinction thresholds for each parameter to be calculated. The model's structure also led to oscillatory behaviour in the long-term. Mosquito populations do experience oscillations in size, but this occurs due to seasonal factors such as rainfall[87, 88], and the oscillations seen in the model often had very short or very long periods, which were unrealistic. This oscillatory behaviour also posed a challenge around how to calculate the average long-term adult population in these model runs (see Supplementary Materials), and using average values fails to accurately represent the differing nature of the oscillations.

Despite these limitations, the model does take into account density-dependent *Anopheles* life-history characteristics that have not previously been widely-included in models of mosquito population dynamics and have not been used before in the field of gene drive research. Furthermore, the model behaves as expected with regards to these density-dependent characteristics and is easily calibrated to different habitat carrying capacities. The model, by incorporating these new density-dependent characteristics, offers key, novel insights into the effectiveness of gene drives, whilst also supporting the work of previous authors[3].

Future Work

It crucial to more accurately model the spread of gene drives. As mentioned above, the way in which a suppression gene-drive is modelled is a simplification of biological inheritance processes, and the model should be extended to explicitly incorporate gene drive dynamics, considering resistance evolution, fitness costs and the homing rate of gene drives. To better assess the efficacy of gene-drive interventions, the model developed in this paper could also be combined with a model for the spatial spread of a gene drive through a mosquito population, such as the those used by North et al.[28] and Eckhoff et al.[39]. This could then be combined with a malaria transmission model, such as malariasimulation[2, 32, 34-37, 89], which would give a more complete understanding of the impact of gene drives on malaria prevalence.

Another avenue of future work that could be pursued is adding a seasonal component to the model, similar to that used by White et al.[2], to better represent the yearly fluctuations in mosquito populations seen in many countries[87, 88, 90]. On the subject of model additions, as discussed above, adding density-dependent larval daily mortality (as well as the already included density-independent larval daily mortality) may better represent experimental findings on density-dependence. This, would, however, significantly complicate Nisbet and Gurney's original model derivation, which relies on larval mortality being independent of time[1]. Regardless of whether seasonality is included in the model (since the level of malaria seasonality varies by country and region[91]), a carrying capacity parameter, for example G_0 in this version of the model, could be used, in combination with a model for malaria transmission, to calibrate the adult *Anopheles* population to the EIR of a specific region or area. This would then allow for the impact of a gene drive in a specific locality to be assessed. Furthermore, since the number of species of *Anopheles* differs by region, incorporating multiple species into the model, and any between-species density dependent effects, could also be an area for future work, as it would again allow better understanding of the impacts of a potential gene-drive programme.

One of the main aims of the project was to investigate the new model's implications for the field of gene-drive research. Extensive modelling work needs to be carried out before gene-drive field trials can start[23], and the work done in this project, combined with the work done using other models for *Anopheles*

mosquito population dynamics, can be used to inform gene-drive field trials and their potential use as a method of malaria control. For example, the smaller impact on malaria transmission suppression suggested by the model developed in this project may mean that larger sample sizes need to be used in field trials. Furthermore, the analysis above suggests that candidate gene drives being tested in laboratory settings may need to render a higher frequency of the population homozygous to achieve the reduction in the number of biting female mosquitoes desired. The project also motivates more experiments on *Anopheles*' density-dependent characteristics in field populations, to better understand the nature of the density dependence.

This project has demonstrated substantial uncertainty around the impact of suppression gene drives on both the number of adult *Anopheles gambiae s.l.* mosquitoes and on the number of biting female mosquitoes. It is therefore important that any work on the impact of a candidate suppression gene drive is conducted using both an ODE-based model, like White et al.'s[(2)], and a DDE-based model like Hancock and Godfray's[(3)]. This would allow the substantial uncertainty around the efficacy of suppression gene drives to be fully understood before any field trials take place. It is also crucial to emphasise this uncertainty, and its impacts on the predicted efficacy of suppression gene drives, when communicating with policy makers. However, it is important to emphasise that modelling work, replete with its simplifications and approximations, is only an estimation of what will happen. It is impossible to know the true impact and implications of introducing a modified gene into the wild before it is introduced, and, in light of the myriad ethical and environmental concerns that surround gene drives, considerable care needs to be taken.

Conclusion

Incorporating density-dependent characteristics into models for *Anopheles gambiae* population dynamics can offer key insights on the effects of important life-history characteristics on possible malaria control interventions. Depending on the model used and the density-dependence assumptions made, the predicted efficacy of interventions that work by reducing mosquito fecundity, such as suppression gene-drives, can vary substantially. More work needs to be done to incorporate a wider range of density-dependent characteristics into robust malaria transmission models. This will then enable the full impact of gene-drive technology to be understood before it is implemented outside the laboratory.

References

1. Nisbet RM, Gurney WSC. The systematic formulation of population models for insects with dynamically varying instar duration. Theoretical Population Biology. 1983;23(1):114-35.
2. White MT, Griffin JT, Churcher TS, Ferguson NM, Basáñez M-G, Ghani AC. Modelling the impact of vector control interventions on Anopheles gambiae population dynamics. Parasites & Vectors. 2011;4(1):153.
3. Hancock PA, Godfray HCJ. Application of the lumped age-class technique to studying the dynamics of malaria-mosquito-human interactions. Malaria Journal. 2007;6(1):98.
4. World Health Organisation. Malaria 2023 [updated 29th March 2023. Available from: https://www.who.int/news-room/fact-sheets/detail/malaria.
5. Bhatt S, Weiss DJ, Cameron E, Bisanzio D, Mappin B, Dalrymple U, et al. The effect of malaria control on Plasmodium falciparum in Africa between 2000 and 2015. Nature. 2015;526(7572):207-11.
6. World Health Organisation. World malaria report 2023. 2023 30/11/2023.
7. World Health Organisation. Global technical strategy for malaria 2016–2030. Geneva; 2015.
8. Sherrard-Smith E, Skarp JE, Beale AD, Fornadel C, Norris LC, Moore SJ, et al. Mosquito feeding behavior and how it influences residual malaria transmission across Africa. Proceedings of the National Academy of Sciences. 2019;116(30):15086-95.
9. Hancock PA, Hendriks CJM, Tangena J-A, Gibson H, Hemingway J, Coleman M, et al. Mapping trends in insecticide resistance phenotypes in African malaria vectors. PLOS Biology. 2020;18(6):e3000633.
10. Malaria Atlas Project. Trends - Malaria - Pf Incidence Rate (Cases per Thousand) [Available from: https://data.malariaatlas.org/trends?year=2020&metricGroup=Malaria&geographicLevel=admin0&metricSubcategory=Pf&metricType=rate&metricName=incidence.
11. Malaria Atlas Project. Trends - Malaria - Pv Incidence Rate (Cases per Thousand) [Available from: https://data.malariaatlas.org/trends?year=2020&metricGroup=Malaria&geographicLevel=admin0&metricSubcategory=Pv&metricType=rate&metricName=incidence.
12. Watson OJ, Gao B, Nguyen TD, Tran TN-A, Penny MA, Smith DL, et al. Pre-existing partner-drug resistance to artemisinin combination therapies facilitates the emergence and spread of artemisinin resistance: a consensus modelling study. The Lancet Microbe. 2022;3(9):e701-e10.
13. Okell LC, Griffin JT, Roper C. Mapping sulphadoxine-pyrimethamine-resistant Plasmodium falciparum malaria in infected humans and in parasite populations in Africa. Sci. 2017;7(1):7389.
14. World Health Organisation. WHO guidelines for malaria - 16 October 2023 2023 [Available from: https://app.magicapp.org/#/guideline/LwRMXj/section/EPMOYj.
15. Sinka ME, Bangs MJ, Manguin S, Rubio-Palis Y, Chareonviriyaphap T, Coetzee M, et al. A global map of dominant malaria vectors. Parasites & Vectors. 2012;5(1):69.
16. Burt A. Site-specific selfish genes as tools for the control and genetic engineering of natural populations. Proc Biol Sci. 2003;270(1518):921-8.
17. Burt A, Koufopanou V. Homing endonuclease genes: the rise and fall and rise again of a selfish element. Current Opinion in Genetics & Development. 2004;14(6):609-15.
18. Hammond A, Galizi R, Kyrou K, Simoni A, Siniscalchi C, Katsanos D, et al. A CRISPR-Cas9 gene drive system targeting female reproduction in the malaria mosquito vector Anopheles gambiae. Nature Biotechnology. 2016;34(1):78-83.
19. Kyrou K, Hammond AM, Galizi R, Kranjc N, Burt A, Beaghton AK, et al. A CRISPR–Cas9 gene drive targeting doublesex causes complete population suppression in caged Anopheles gambiae mosquitoes. Nature Biotechnology. 2018;36(11):1062-6.
20. Carballar-Lejarazú R, Dong Y, Pham TB, Tushar T, Corder RM, Mondal A, et al. Dual effector population modification gene-drive strains of the African malaria mosquitoes, Anopheles gambiae and Anopheles coluzzii. Proc Natl Acad Sci U S A. 2023;120(29):e2221118120.
21. Dhole S, Lloyd AL, Gould F. Gene Drive Dynamics in Natural Populations: The Importance of Density Dependence, Space, and Sex. Annual Review of Ecology, Evolution, and Systematics. 2020;51(1):505-31.
22. National Academies of Sciences, Engineering and Medicine. Gene Drives on the Horizon: Advancing Science, Navigating Uncertainty, and Aligning Research with Public Values. Washington, DC: National Academies Press; 2016.
23. World Health Organisation. Guidance framework for testing of genetically modified mosquitoes, second edition. 2021.
24. Connolly JB, Mumford JD, Fuchs S, Turner G, Beech C, North AR, Burt A. Systematic identification of plausible pathways to potential harm via problem formulation for investigational releases of a population suppression gene drive to control the human malaria vector Anopheles gambiae in West Africa. Malaria Journal. 2021;20(1):170.
25. Depinay J-MO, Mbogo CM, Killeen G, Knols B, Beier J, Carlson J, et al. A simulation model of African Anopheles ecology and population dynamics for the analysis of malaria transmission. Malaria Journal. 2004;3(1):29.
26. Clements AN. The biology of mosquitoes. Wallingford: CABI; 2000. 511 p.
27. North AR, Godfray HCJ. Modelling the persistence of mosquito vectors of malaria in Burkina Faso. Malaria Journal. 2018;17(1):140.
28. North AR, Burt A, Godfray HCJ. Modelling the suppression of a malaria vector using a CRISPR-Cas9 gene drive to reduce female fertility. BMC Biology. 2020;18(1):98.
29. Deredec A, Godfray HC, Burt A. Requirements for effective malaria control with homing endonuclease genes. Proc Natl Acad Sci U S A. 2011;108(43):E874-80.
30. Sánchez C. HM, Wu SL, Bennett JB, Marshall JM. MGDrivE: A modular simulation framework for the spread of gene drives through spatially explicit mosquito populations. Methods in Ecology and Evolution. 2020;11(2):229-39.

31. Marshall JM, Buchman A, Sánchez CH, Akbari OS. Overcoming evolved resistance to population-suppressing homing-based gene drives. Sci Rep. 2017;7(1):3776.
32. Griffin JT, Hollingsworth TD, Okell LC, Churcher TS, White M, Hinsley W, et al. Reducing Plasmodium falciparum Malaria Transmission in Africa: A Model-Based Evaluation of Intervention Strategies. PLOS Medicine. 2010;7(8):e1000324.
33. Griffin JT, Ferguson NM, Ghani AC. Estimates of the changing age-burden of Plasmodium falciparum malaria disease in sub-Saharan Africa. Nat Commun. 2014;5:3136.
34. Okell LC, Cairns M, Griffin JT, Ferguson NM, Tarning J, Jagoe G, et al. Contrasting benefits of different artemisinin combination therapies as first-line malaria treatments using model-based cost-effectiveness analysis. Nat Commun. 2014;5:5606.
35. Griffin JT, Bhatt S, Sinka ME, Gething PW, Lynch M, Patouillard E, et al. Potential for reduction of burden and local elimination of malaria by reducing Plasmodium falciparum malaria transmission: a mathematical modelling study. Lancet Infect Dis. 2016;16(4):465-72.
36. Winskill P, Slater HC, Griffin JT, Ghani AC, Walker PGT. The US President's Malaria Initiative, Plasmodium falciparum transmission and mortality: A modelling study. PLOS Medicine. 2017;14(11):e1002448.
37. Sherrard-Smith E, Griffin JT, Winskill P, Corbel V, Pennetier C, Djénontin A, et al. Systematic review of indoor residual spray efficacy and effectiveness against Plasmodium falciparum in Africa. Nature Communications. 2018;9(1):4982.
38. Wu SL, Bennett JB, Sánchez CH, Dolgert AJ, León TM, Marshall JM. MGDrivE 2: A simulation framework for gene drive systems incorporating seasonality and epidemiological dynamics. PLoS Comput Biol. 2021;17(5):e1009030.
39. Eckhoff PA, Wenger EA, Godfray HC, Burt A. Impact of mosquito gene drive on malaria elimination in a computational model with explicit spatial and temporal dynamics. Proc Natl Acad Sci U S A. 2017;114(2):E255-e64.
40. Eckhoff PA. A malaria transmission-directed model of mosquito life cycle and ecology. Malar J. 2011;10:303.
41. McCarthy KA, Wenger EA, Huynh GH, Eckhoff PA. Calibration of an intrahost malaria model and parameter ensemble evaluation of a pre-erythrocytic vaccine. Malaria Journal. 2015;14(1):6.
42. Metchanun N, Borgemeister C, Amzati G, von Braun J, Nikolov M, Selvaraj P, Gerardin J. Modeling impact and cost-effectiveness of driving-Y gene drives for malaria elimination in the Democratic Republic of the Congo. Evolutionary Applications. 2022;15(1):132-48.
43. Beaghton A, Beaghton PJ, Burt A. Gene drive through a landscape: Reaction-diffusion models of population suppression and elimination by a sex ratio distorter. Theor Popul Biol. 2016;108:51-69.
44. Beaghton A, Beaghton PJ, Burt A. Vector control with driving Y chromosomes: modelling the evolution of resistance. Malar J. 2017;16(1):286.
45. Huang Y, Magori K, Lloyd AL, Gould F. Introducing desirable transgenes into insect populations using Y-linked meiotic drive - a theoretical assessment. Evolution. 2007;61(4):717-26.
46. Deredec A, Burt A, Godfray HC. The population genetics of using homing endonuclease genes in vector and pest management. Genetics. 2008;179(4):2013-26.
47. Sumba LA, Ogbunugafor CB, Deng AL, Hassanali A. Regulation of oviposition in Anopheles gambiae s.s.: role of inter- and intra-specific signals. J Chem Ecol. 2008;34(11):1430-6.
48. Lyimo EO, Takken W, Koella JC. Effect of rearing temperature and larval density on larval survival, age at pupation and adult size of Anopheles gambiae. Entomologia Experimentalis et Applicata. 1992;63(3):265-71.
49. Schneider P, Takken W, Mccall PJ. Interspecific competition between sibling species larvae of Anopheles arabiensis and An. gambiae. Medical and Veterinary Entomology. 2000;14(2):165-70.
50. Tchuinkam T, Mpoame M, Make-Mveinhya B, Simard F, Lélé-Defo E, Zébazé-Togouet S, et al. Optimization of breeding output for larval stage of Anopheles gambiae (Diptera: Culicidae): prospects for the creation and maintenance of laboratory colony from wild isolates. Bull Entomol Res. 2011;101(3):259-69.
51. Gilles JR, Lees RS, Soliban SM, Benedict MQ. Density-dependent effects in experimental larval populations of Anopheles arabiensis (Diptera: Culicidae) can be negative, neutral, or overcompensatory depending on density and diet levels. J Med Entomol. 2011;48(2):296-304.
52. Tsila H, Messi J, Foko D. Adaptative Responses of Anopheles gambiae in Crowding Larvae Conditions in Laboratory. Asian Journal of Biological Sciences. 2011;4:259-65.
53. Yadav R, Tyagi V, Sharma A, Tikar S, Sukumaran D, Veer V. Overcrowding Effects on Larval Development of Four Mosquito Species Aedes Albopictus, Aedes Aegypti, Culex Quinquefasciatus and Anopheles Stephensi. International Journal of Research Studies in Zoology. 2017;3:1-10.
54. Ng'habi KR, John B, Nkwengulila G, Knols BGJ, Killeen GF, Ferguson HM. Effect of larval crowding on mating competitiveness of Anopheles gambiae mosquitoes. Malaria Journal. 2005;4(1):49.
55. Timmermann SE, Briegel H. Water depth and larval density affect development and accumulation of reserves in laboratory populations of mosquitoes. Bulletin of the Society of Vector Ecologists. 1993;18(2):174-87.
56. Njunwa K. Studies on the productivity of 'Anopheles' breeding sites in relation to adult mosquito density [Doctoral]: London School of Hygiene & Tropical Medicine; 1993.
57. Gimnig JE, Ombok M, Otieno S, Kaufman MG, Vulule JM, Walker ED. Density-Dependent Development of Anopheles gambiae (Diptera: Culicidae) Larvae in Artificial Habitats. Journal of Medical Entomology. 2002;39(1):162-72.
58. Muriu SM, Coulson T, Mbogo CM, Godfray HCJ. Larval density dependence in Anopheles gambiae s.s., the major African vector of malaria. Journal of Animal Ecology. 2013;82(1):166-74.
59. Russell TL, Burkot TR, Bugoro H, Apairamo A, Beebe NW, Chow WK, et al. Larval habitats of the Anopheles farauti and Anopheles lungae complexes in the Solomon Islands. Malaria Journal. 2016;15(1):164.
60. Munga S, Minakawa N, Zhou G, Mushinzimana E, Barrack OO, Githeko AK, Yan G. Association between land cover and habitat productivity of malaria vectors in western Kenyan highlands. Am J Trop Med Hyg. 2006;74(1):69-75.

61. Bayoh MN, Lindsay SW. Effect of temperature on the development of the aquatic stages of Anopheles gambiae sensu stricto (Diptera: Culicidae). Bull Entomol Res. 2003;93(5):375-81.
62. Kirby MJ, Lindsay SW. Effect of temperature and inter-specific competition on the development and survival of Anopheles gambiae sensu stricto and An. arabiensis larvae. Acta Tropica. 2009;109(2):118-23.
63. Takken W, Klowden MJ, Chambers GM. Effect of body size on host seeking and blood meal utilization in Anopheles gambiae sensu stricto (Diptera: Culicidae): the disadvantage of being small. J Med Entomol. 1998;35(5):639-45.
64. Russell T, Lwetoijera D, Knols B, Takken W, Killeen G, Ferguson H. Linking individual phenotype to densitydependent population growth: The influence of body size on the population dynamics of malaria vectors. Proceedings Biological sciences / The Royal Society. 2011;278:3142-51.
65. Ngowo HS, Okumu FO, Hape EE, Mshani IH, Ferguson HM, Matthiopoulos J. Using Bayesian state-space models to understand the population dynamics of the dominant malaria vector, Anopheles funestus in rural Tanzania. Malaria Journal. 2022;21(1):161.
66. Koella JC, Lyimo EO. Variability in the Relationship Between Weight and Wing Length of Anopheles gambiae (Diptera: Culicidae). Journal of Medical Entomology. 1996;33(2):261-4.
67. Lyimo EO, Takken W. Effects of adult body size on fecundity and the pre-gravid rate of Anopheles gambiae females in Tanzania. Med Vet Entomol. 1993;7(4):328-32.
68. Service MW. Studies on sampling larval populations of the Anopheles gambiae complex. Bull World Health Organ. 1971;45(2):169-80.
69. Service MW. Mortalities of the larvae of the Anopheles gambiae Giles complex and detection of predators by the precipitin test. Bulletin of Entomological Research. 1973;62(3):359-69.
70. Service MW. Mortalities of the immature stages of species B of the Anopheles gambiae complex in Kenya: comparison between rice fields and temporary pools, identification of predators, and effects of insecticidal spraying. J Med Entomol. 1977;13(4-5):535-45.
71. Centers for Diseas Control and Prevention. Malaria - About Malaria - Biology - Mosquitoes 2020 [Available from: https://www.cdc.gov/malaria/about/biology/index.html.
72. R Core Team. R: A Language and Environment for Statistical Computing. 4.3.2 ed. Vienna, Austria: R Foundation for Statistical Computing; 2023.
73. FitzJohn R. odin: ODE Generation and Integration. 1.2.5 ed2023.
74. Wickham H, François R, Henry L, Müller K, Vaughan D. dplyr: A Grammar of Data Manipulation. 1.1.3 ed2023.
75. Wickham H. ggplot2: Elegant Graphics for Data Analysis: Springer-Verlag New York; 2016.
76. Wickham H, Averick M, Bryan J, Chang W, McGowan LDA, François R, et al. Welcome to the tidyverse. Journal of Open Source Software. 2019;4:1686.
77. Mills BR. MetBrewer: Color Palettes Inspired by Works at the Metropolitan Museum of Art. 0.3.0 ed2023.
78. Wickham H, Pedersen TL, Seidel D. scales: Scale Functions for Visualization. 1.2.1 ed2023.
79. Arnold JB. ggthemes: Extra Themes, Scales and Geoms for 'ggplot2'. 4.2.4 ed2023.
80. Pedersen TL. patchwork: The Composer of Plots. 1.1.3 ed2023.
81. Soetaert K. rootSolve: Nonlinear root finding, equilibrium and steady-state analysis of ordinary differential equations. R package 1.6 ed2009.
82. Orondo PW, Zhou G, Ochwedo KO, Wang X, Ondeto BM, Lee M-C, et al. Effect of predators on Anopheles arabiensis and Anopheles funestus larval survivorship in Homa Bay County Western Kenya. Malaria Journal. 2023;22(1):298.
83. Stephens PA, Sutherland WJ, Freckleton RP. What Is the Allee Effect? Oikos. 1999;87(1):185-90.
84. Koenraadt CJ, Takken W. Cannibalism and predation among larvae of the Anopheles gambiae complex. Med Vet Entomol. 2003;17(1):61-6.
85. Bayoh MN, Lindsay SW. Temperature-related duration of aquatic stages of the Afrotropical malaria vector mosquito Anopheles gambiae in the laboratory. Med Vet Entomol. 2004;18(2):174-9.
86. Yaro AS, Dao A, Adamou A, Crawford JE, Ribeiro JMC, Gwadz R, et al. The distribution of hatching time in Anopheles gambiae. Malaria Journal. 2006;5(1):19.
87. Koenraadt CJ, Githeko AK, Takken W. The effects of rainfall and evapotranspiration on the temporal dynamics of Anopheles gambiae s.s. and Anopheles arabiensis in a Kenyan village. Acta Trop. 2004;90(2):141-53.
88. Kabbale FG, Akol AM, Kaddu JB, Onapa AW. Biting patterns and seasonality of anopheles gambiae sensu lato and anopheles funestus mosquitoes in Kamuli District, Uganda. Parasites & Vectors. 2013;6(1):340.
89. Griffin JT, Ferguson NM, Ghani AC. Estimates of the changing age-burden of Plasmodium falciparum malaria disease in sub-Saharan Africa. Nature Communications. 2014;5(1):3136.
90. Whittaker C, Winskill P, Sinka M, Pironon S, Massey C, Weiss DJ, et al. A novel statistical framework for exploring the population dynamics and seasonality of mosquito populations. Proc Biol Sci. 2022;289(1972):20220089.
91. Cairns ME, Walker PGT, Okell LC, Griffin JT, Garske T, Asante KP, et al. Seasonality in malaria transmission: implications for case-management with long-acting artemisinin combination therapy in sub-Saharan Africa. Malaria Journal. 2015;14(1):321.

Supplementary Materials

Nisbet and Gurney's original model with an added pupal class

Adding only a pupal class (keeping fecundity constant) to Nisbet and Gurney's original model gives the following set of DDEs:

$$\frac{dF(t)}{dt} = G_0 - \frac{A_{max}L(t)F(t)}{K_F + F(t)} \tag{50}$$

$$\frac{dL(t)}{dt} = \frac{qN(t)}{2} - \frac{qN\left(t-\tau_L(t)\right)}{2} e^{-\mu_L\tau_L(t)} \frac{F(t)\left(K_F + F\left(t-\tau_L(t)\right)\right)}{F\left(t-\tau_L(t)\right)\left(K_F + F(t)\right)} - \mu_L L(t) \tag{51}$$

$$\frac{\mathrm{dP(t)}}{\mathrm{dt}} = \frac{qN\left(t-\tau_L(t)\right)}{2} e^{-\mu_L\tau_L(t)} \frac{F(t)\left(K_F + F\left(t-\tau_L(t)\right)\right)}{F\left(t-\tau_L(t)\right)\left(K_F + F(t)\right)} - \frac{P(t)}{\tau_P} - \mu_P P(t) \tag{52}$$

$$\frac{dN(t)}{dt} = I_N(t) + \frac{P(t)}{\tau_P} - \mu_N N(t) \tag{53}$$

$$\frac{d\tau_L(t)}{dt} = 1 - \frac{F(t)\left(K_F + F\left(t-\tau_L(t)\right)\right)}{F\left(t-\tau_L(t)\right)\left(K_F + F(t)\right)} \tag{54}$$

with initial conditions:

$$F(t) = F_0 \; \forall \; t \leq 0 \tag{55}$$

$$L(t) = 0 \; \forall \; t \leq 0 \tag{56}$$

$$P(t) = 0 \; \forall \; t \leq 0 \tag{57}$$

$$N(t) = 0 \; \forall \; t \leq 0 \tag{58}$$

$$\tau_L(t) = \frac{m_p(K_F + F_0)}{\gamma A_{max} F_0} \; \forall \; t \leq 0 \tag{59}$$

and equilibrium solution:

$$F* = \frac{K_F m_P \mu_L}{\gamma A_{max} \log\left(\frac{q}{2\mu_N(1+\mu_P\tau_P)}\right) - m_P\mu_L} \tag{60}$$

$$L* = \frac{G_0 \gamma \log\left(\frac{q}{2\mu_N(1+\mu_P\tau_P)}\right)}{m_P\mu_L} \tag{61}$$

$$P* = \frac{2\mu_N\tau_P G_0 \gamma \log\left(\frac{q}{2\mu_N(1+\mu_P\tau_P)}\right)}{m_P\left(q - 2\mu_N(1+\mu_P\tau_P)\right)} \tag{62}$$

$$N* = \frac{2G_0 \gamma \log\left(\frac{q}{2\mu_N(1+\mu_P\tau_P)}\right)}{m_P\left(q - 2\mu_N(1+\mu_P\tau_P)\right)} \tag{63}$$

$$\tau_L* = \frac{1}{\mu_L}\log\left(\frac{q}{2\mu_N(1+\mu_P\tau_P)}\right) \tag{64}$$

where $L*$, $F*$, $P*$, $N*$ and τ_L* are the values of $L(t)$, $F(t)$, $P(t)$, $N(t)$ and $\tau_L(t)$ at equilibrium. The derivation for this equilibrium solution is included below.

Just as with Nisbet and Gurney's original model, we have a condition for the steady state above to be physical. We require that:

$$\gamma A_{max} \log\left(\frac{q}{2\mu_N(1+\mu_P\tau_P)}\right) > m_P\mu_L \tag{65}$$

which is equivalent to the second condition of Nisbet and Gurney's original model.

Derivation of the Equilibrium Solution of Nisbet and Gurney's original model with an added pupal class but constant fecundity

As Nisbet and Gurney set out[1], we analyse the equilibrium solutions of the system after the initial injection of adult mosquitoes, i.e. after time T_1, which allows us to set $I_N(t) = 0$. At equilibrium, all time-dependent variables are constant, and their rates of change are equal to 0, meaning that, at equilibrium, (50) - (54) give us the following set of equations:

$$G_0 = \frac{A_{max} L* F*}{K_F + F*} \tag{66}$$

$$P* = \mu_N \tau_P N* \tag{67}$$

$$P* \left(\frac{1}{\tau_P} + \mu_P\right) = \frac{qN*}{2} e^{-\mu_L \tau_{L^*}} \tag{68}$$

$$L* = \frac{qN*}{2\mu_L}(1 - e^{-\mu_L \tau_{L^*}}) \tag{69}$$

Substituting (67) into (68) gives:

$$\mu_N \tau_P N* \left(\frac{1}{\tau_P} + \mu_P\right) = \frac{qN*}{2} e^{-\mu_L \tau_{L^*}} \tag{70}$$

$$\Rightarrow \quad N* \left(\mu_N(1 + \mu_P \tau_P) - \frac{q}{2} e^{-\mu_L \tau_{L^*}}\right) = 0 \tag{71}$$

This equation has two solutions, one of which is $N* = 0$. If $N* = 0$, we must also have that $L* = 0$ (from (69)), which is a contradiction as $G_0 \neq 0$. Therefore, the only solution to (71) is:

$$\frac{q}{2} e^{-\mu_L \tau_{L^*}} = \mu_N(1 + \mu_P \tau_P) \tag{72}$$

$$\Rightarrow \tau_L* = \frac{1}{\mu_L} ln\left(\frac{q}{2\mu_N(1 + \mu_P \tau_P)}\right) \tag{73}$$

Following Nisbet and Gurney[1], we also use that at equilibrium, we have:

$$m_P = \int_{t-\tau_L(t)}^{t} g_L(t')dt' = \int_{t-\tau_L(t)}^{t} \frac{\gamma A_{max} F(t')}{K_F + F(t')} dt' = \int_{t-\tau_{L^*}}^{t} \frac{\gamma A_{max} F*}{K_F + F*} dt' = \frac{\gamma A_{max} F* \tau_L*}{K_F + F*} \tag{74}$$

$$\Rightarrow F* = \frac{K_F}{\frac{\gamma A_{max} \tau_L*}{m_P} - 1} \tag{75}$$

Equations (66)-(67), (69), (73) and (75) then give us our full equilibrium solutions (equations (60) - (64)).

Alternative Density-dependent Fecundity Equation

An alternative way to model density-dependent fecundity is to assume a simple exponential relationship between fecundity and larval development time. This meant that our new fecundity term, $\tilde{q}(t)$, could be written as:

$$\tilde{q}(t) = \kappa \mathrm{e}^{-\lambda(\tau_L(t-\tau_P)-5)} \tag{76}$$

where κ and λ are constants that determine the shape of the relationship. Modelling $\tilde{q}(t)$ in this way is advantageous, as with this formulation the model has an analytical equilibrium solution, which can be found in the same way as for the model formulations described above. However, this relationship between fecundity and larval development time is less accurate when compared with the relationship seen in experimental studies.

Analysis of the Updated Model with an alternative density-dependent fecundity equation

Nisbet and Gurney's model with an added pupal class and with the density-dependent fecundity relationship above has an analytically-derivable equilibrium solution, which can be derived in a similar way to the equilibrium solutions for both Nisbet and Gurney's original model (which is presented in Appendix 2 of their 1993 paper[1]) and the intermediary version of Nisbet and Gurney's model presented above, which includes a pupal class but still has constant fecundity. The equilibrium solution for this model is:

$$F* = \frac{K_F m_P(\mu_L + \lambda)}{\gamma A_{max}\left(\log\left(\frac{\kappa}{\mu_N(1+\mu_P\tau_P)}\right) + 5\lambda\right) - m_P(\mu_L+\lambda)} \tag{77}$$

$$L* = \frac{G_0\gamma\left(\log\left(\frac{\kappa}{\mu_N(1+\mu_P\tau_P)}\right) + 5\lambda\right)}{m_P(\mu_L+\lambda)} \tag{78}$$

$$P* = \frac{\mu_N\tau_P\mu_L G_0\gamma\left(\log\left(\frac{\kappa}{\mu_N(1+\mu_P\tau_P)}\right) + 5\lambda\right)}{m_P(\mu_L+\lambda)\left(\left(\kappa^{\mu_L}e^{5\mu_L\lambda}\left(\mu_N(1+\mu_P\tau_P)\right)^{\lambda}\right)^{\frac{1}{\mu_L+\lambda}} - \mu_N(1+\mu_P\tau_P)\right)} \tag{79}$$

$$N* = \frac{\mu_L G_0 \gamma \left(\log\left(\frac{\kappa}{\mu_N(1+\mu_P\tau_P)}\right) + 5\lambda\right)}{m_P(\mu_L+\lambda)\left(\left(\kappa^{\mu_L} e^{5\mu_L\lambda}\left(\mu_N(1+\mu_P\tau_P)\right)^{\lambda}\right)^{\frac{1}{\mu_L+\lambda}} - \mu_N(1+\mu_P\tau_P)\right)} \tag{80}$$

$$\tau_L* = \frac{\log\left(\frac{\kappa}{\mu_N(1+\mu_P\tau_P)}\right) + 5\lambda}{\mu_L+\lambda} \tag{81}$$

which provides us with three conditions that must be satisfied if this solution is to be physical:

$$\kappa > \mu_N(1+\mu_P\tau_P) \tag{82}$$

$$\gamma A_{max}\left(\log\left(\frac{\kappa}{\mu_N(1+\mu_P\tau_P)}\right) + 5\lambda\right) > m_P(\mu_L+\lambda) \tag{83}$$

$$\left(\kappa^{\mu_L} e^{5\mu_L\lambda}\left(\mu_N(1+\mu_P\tau_P)\right)^{\lambda}\right)^{\frac{1}{\mu_L+\lambda}} > \mu_N(1+\mu_P\tau_P) \tag{84}$$

Here (82) comes from equation (81), (83) from equation (77) and (84) from equation (80).

Expanding (84) gives us, after some rearrangement, the following formula:

$$\left(\frac{ke^{5\lambda}}{\mu_N(1+\mu_P\tau_P)}\right)^{\frac{\mu_L}{\mu_L+\lambda}} > 1 \tag{85}$$

and therefore, as λ is a positive constant, if (82) is true then so is (84). This leaves us with 2 conditions for physicality, (82) and (83). However, in practice, as long as the minimum larval to pupal development time is assumed to be greater than or equal to 5, then the RHS of equation (86) below, a rearrangement of (83), is always positive (as we have, from equation (8), that $\tau_{L_{min}} = \frac{m_P}{\gamma A_{max}}$).

$$\log\left(\frac{\kappa}{\mu_N(1+\mu_P\tau_P)}\right) > \frac{m_P}{\gamma A_{max}}\mu_L + \left(\frac{m_P}{\gamma A_{max}} - 5\right)\lambda \tag{86}$$

As a result, we can see that (82) is necessary for (83), meaning that, as with Nisbet and Gurney's model, satisfying just one condition, equation (83), will lead to a physical (non-negative) equilibrium solution.

The model was not stable for all parameter values used, and exhibited both limit cycles and population extinction. The points at which this qualitative change in stability occurred for each parameter value was calculated, and it was found that the conditions for the physicality of the steady state (i.e. equation (83), or possibly equations (82) and (83)) also determined whether the population of larvae, pupae and adults became extinct. This makes sense; since it is impossible to have a negative quantity of food or number of mosquitoes, in the region of the parameter space for which the equilibrium solution of the model would be unphysical, the analytically-derivable steady state is unstable, and instead the *Anopheles* population tends to zero, whilst the quantity of food in the system escapes to infinity (since food always enters the system at a constant rate, and if there are no larvae to consume it, then the amount increases linearly).

Algorithm used to classify the equilibrium solution of the Modified Nisbet and Gurney model used in the project and to calculate the long-term value of its states

If the model hadn't become extinct or reached a stable equilibrium by day 18250, but the amount of food in the system had been monotonically increasing since day 1000 of the model run, the model was run again over a longer time frame for those parameter values, as this implied that the larval, pupal, and adult states were progressing towards extinction but had not yet reached that point. The model was run for 10 times longer (i.e. 182500 days), and the method for assessing whether the model had reached equilibrium or extinction detailed in Methods was repeated. This process was repeated until all 3 states (larval, pupal, and adult) had reached extinction, which in practice meant that the model did not have to be run for more than 5000 years post-adult-introduction.

If the food in the system had not been increasing monotonically since day 1000, the value of each state at its last and third-last maxima was calculated, as the model was assumed to be exhibiting oscillatory behaviour. If the value of the state at its third-last maxima was within 0.5% of its value at the last maxima, and the final three maxima all occurred after day 1000, it was assumed that the model was exhibiting regularly sized oscillations, and the mean of each state between these two maxima (which was either one or two periods of the oscillation) was calculated and taken as the long-term value of that state. Otherwise, the model was run again over a longer time-frame. In these cases, the model was run for 10 times longer

for those parameter values, and the pre-defined threshold for the oscillations to have stabilised was doubled (i.e. to 1% and then to 2%). This process was repeated until the oscillations of the states being studied had stabilised, though again, for the states being examined, the model did not need to be run for more than 5000 years post-initialisation.

Parameter values used in the model comparison

Parameter	Description	Unit	Value	Source
μ_{E_0}	Per-capita death rate of early-stage larvae (1st and 2nd instars)	day^{-1}	0.034	Posterior from White et al.[2]
μ_{L_0}	Per-capita death rate of late-stage larvae (3rd and 4th instars)	day^{-1}	0.035	Posterior from White et al.[2]
$\mu_{P_{White}}$	Per-capita death rate of pupae	day^{-1}	0.25	Posterior from White et al.[2]
$\mu_{N_{White}}$	Per-capita death rate of adults	day^{-1}	0.096	Posterior from White et al.[2]
d_E	Development time of early-stage larvae	day	6.64	Posterior from White et al.[2]
d_L	Development time of late-stage larvae	day	3.72	Posterior from White et al.[2]
$\tau_{P_{White}}$	Development time of pupae	day	0.64	Posterior from White et al.[2]
β	Eggs successfully hatched per female mosquito per day	day^{-1}	21.19	Posterior from White et al.[2]
γ_W	"Effect of density dependence on late instars relative to early instars"	-	0.395	Posterior from White et al.[2]
K_W	Larval carrying capacity	larvae	1000	Arbitrary

Table A1: Parameter values used in White et al.'s model[2] for model comparison.

Parameter	Description	Unit	Value	Source
μ_0	Per-capita death rate of eggs	day^{-1}	0.05	Hancock and Godfray[3]
$\mu_{L_{HG}}$	Per-capita death rate of larvae	day^{-1}	0.1	Hancock and Godfray[3]
$\mu_{P_{HG}}$	Per-capita death rate of pupae	day^{-1}	0.05	Hancock and Godfray[3]
$\mu_{N_{HG}}$	Per-capita death rate of adults	day^{-1}	0.1	Hancock and Godfray[3]
t_0	Development time of eggs	day	1	Hancock and Godfray[3]
t_L	Development time of larvae	day	14	Hancock and Godfray[3]
$\tau_{P_{HG}}$	Development time of pupae	day	1	Hancock and Godfray[3]
q_0	Eggs laid per female mosquito per day	day^{-1}	30	Hancock and Godfray[3]
γ_{HG}	Parameter related to density dependence that also controls carrying capacity	day^{-1}area^2	1.161254×10^{-5}	Set so the equilibrium number of larvae in Hancock and Godfray's model[3] matches White et al.'s[2] equilibrium number of larvae with the parameter values above and in Table A1

Table A2: Parameter values used in Hancock and Godrfay's model[26] for model comparison.

Supplementary Figures

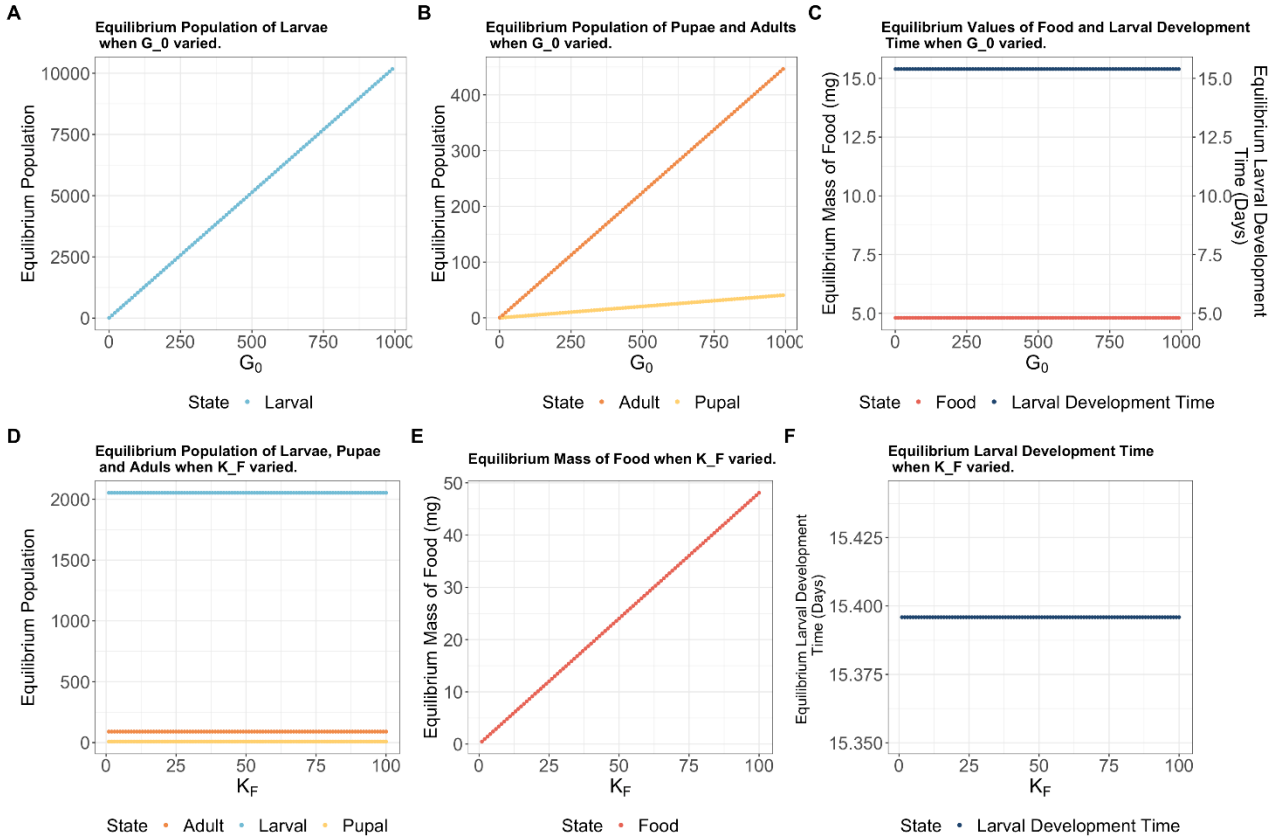

Figure A1: Equilibrium values of the model's states when varying either G_0 (top row) or K_F (bottom row), with all other parameters kept at their default values.

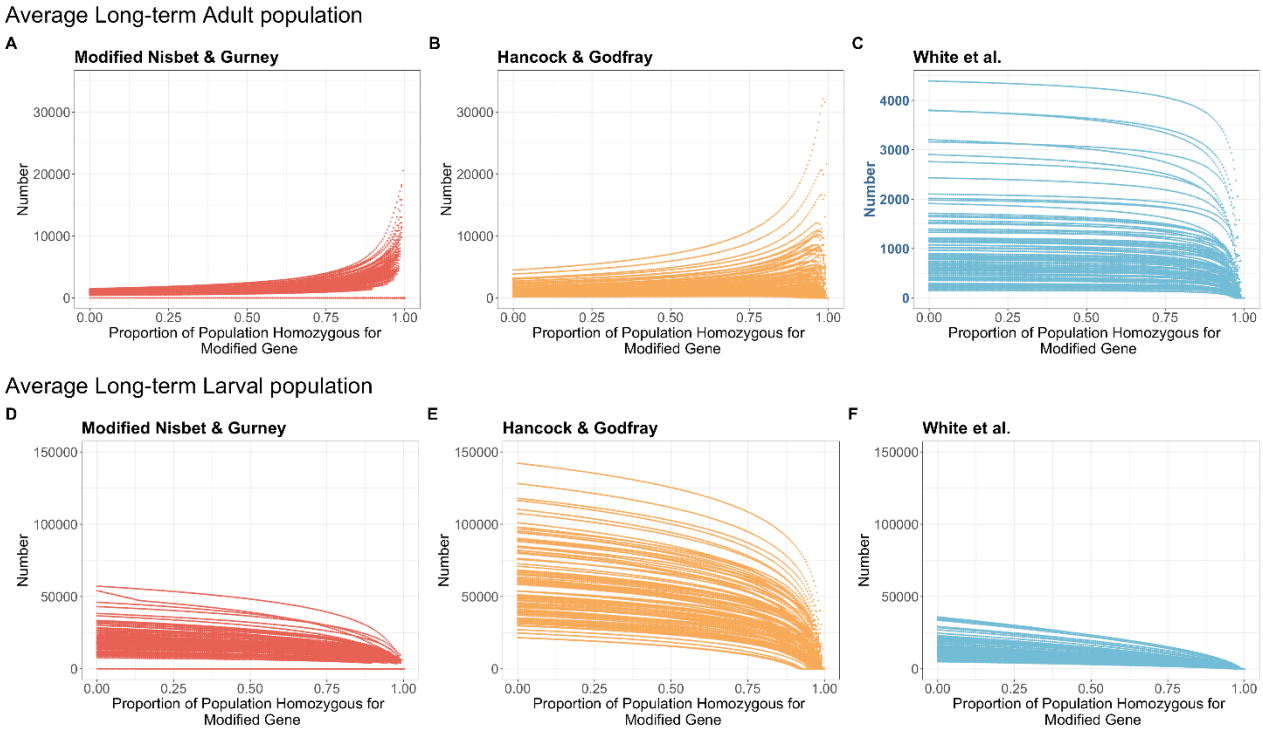

Figure A2: Long-term adult (top row) and larval (bottom row) Anopheles mosquito population sizes for varying fecundity for the 100 Latin Hypercube samples of each parameter (excluding fecundity and carrying-capacity-related parameters) from the three different models for mosquito population dynamics: the Modified Nisbet and Gurney model from this paper (leftmost column, plots A and D), the Hancock and Godfray (2007) model (middle column, plots B and E) and White et al.'s (2011) model (rightmost column, plots C and F). The blue y-axis labels on plot C indicate that it has a different range to plots A & B, which both have the same y-axis range. Plots D,E & F all have the same y-axis range.